Plant Physiology Preview. Published on October 26, 2018, as DOI:10.1104/pp.18.01006

Short title: On the composite nature of water flow in roots

Corresponding author: xavier.draye@uclouvain.be (tel.: +32 10 472092)

Going with the flow: multiscale insights into the composite nature of water transport in roots

Valentin Couvreur[1], Marc Faget[1], Guillaume Lobet[1,3], Mathieu Javaux[2,3], François Chaumont[4] and Xavier Draye[1]

[1] Earth and Life Institute, Agronomy, Université catholique de Louvain, 1348 Louvain-la-Neuve, Belgium

[2] Earth and Life Institute, Environmental Sciences, Université catholique de Louvain, 1348 Louvain-la-Neuve, Belgium

[3] Forschungszentrum Juelich GmbH, IBG3 Agrosphere, Juelich, Germany

[4] Louvain Institute of Biomolecular Science and Technology, Université catholique de Louvain, 1348 Louvain-la-Neuve, Belgium

Author contributions: V.C. and M.F. developed the MECHA code; G.L. developed the ShinyApp; V.C. wrote the article with contributions of all the authors; X.D. supervised the research and conceived the original screening and research plans.

One-sentence summary: A bio-physical model of the "root hydraulic anatomy" allows testing hypotheses related to radial water transport down to the cell level and proves complementary to current experimental approaches.

Word count: Introduction (1548), Results (1554), Discussion (1743), Conclusion (512), Methods (2421), Acknowledgements (122), Total (7900).

Number of figures: 6 (colours)

Number of tables: 3

Supporting information: 5 Notes, 3343 words, 5 figures (colours)

Abstract:

As water often limits crop production, a more complete understanding of plant water capture and transport is necessary. Here, we developed MECHA, a mathematical model that computes the flow of water across the root at the scale of walls, membranes, and plasmodesmata of individual cells, and used it to test hypotheses related to root water transport in maize (*Zea mays*). The model uses detailed root anatomical descriptions and a minimal set of experimental cell properties, including the conductivity of plasma membranes (L_p), cell walls, and plasmodesmata, which yield quantitative and scale consistent estimations of water pathways and root radial hydraulic conductivity (k_r). MECHA revealed that the mainstream hydraulic theories derived independently at the cell and root segment scales are compatible only if osmotic potentials within the apoplastic domains are uniform. Results suggested that the convection-diffusion of apoplastic solutes explained most of the offset between estimated k_r in pressure clamp and osmotic experiments, while the contribution of water-filled intercellular spaces was limited. Furthermore, sensitivity analyses quantified the relative impact of cortex and endodermis cell L_p on root k_r and suggested that only the latter substantially contributed to k_r due to the composite nature of water flow across roots. The explicit root hydraulic anatomy framework brings insights into contradictory interpretations of experiments from the literature and suggests experiments to efficiently address questions pertaining to root water relations. Its scale-consistency opens avenues for cross-scale communication in the world of root hydraulics.

Keywords: Aquaporins, Cell hydraulics modelling, Composite pathways, Multiscale, Plasmodesmata, Root anatomy, *Zea mays*.

Symbols: K_{PD}: individual plasmodesmata hydraulic conductance, k_r: root radial hydraulic conductivity, k_w: cell primary wall hydraulic conductivity, L_p: cell plasma membrane hydraulic conductivity, σ: cell membrane reflection coefficient, σ_r: root reflection coefficient

Introduction

Worldwide crop production is frequently limited by situations where the water supply is lower than the crop evaporative demand (Cattivelli *et al.*, 2008). To develop crops and crop management systems that maintain high yields under water limited conditions, we need a clear understanding of the variables and processes which control root water capture and plant water use. Root water uptake is largely influenced by the hydraulic properties of the soil-root network (Sperry *et al.*, 2002; Draye *et al.*, 2010; Schoppach *et al.*, 2014). Among these properties, the root radial conductivity (k_r) stands out as a central feature (Parent *et al.*, 2009; Draye *et al.*, 2010). It reportedly responds within hours to its hydric environment (Hachez *et al.*, 2012; Caldeira *et al.*, 2014), allowing rapid adjustments of xylem water status and flow rates between soil and roots (Meunier *et al.*, 2017b).

There is growing evidence that sub-cellular components, such as water channels (aquaporins) and plasmodesmata, contribute to the regulation of k_r (Steudle & Peterson, 1998; Parent *et al.*, 2009). On the one hand, the abundance and conformation of aquaporins control "transmembrane" elements of water pathways via cell membrane permeability (L_p) (Maurel & Chrispeels, 2001; Chaumont & Tyerman, 2014). The gating of aquaporins provokes k_r reductions of -60% to -70% (Ye & Steudle, 2006; Boursiac *et al.*, 2008; Parent *et al.*, 2009). On the other hand, the aperture and frequency of plasmodesmata, which connect the protoplasts of adjacent cells (Maule, 2008; Sevilem *et al.*, 2013; Brunkard & Zambryski, 2017), regulates "symplastic" elements of water pathways. Additionally, hydrophobic substances such as lignin (e.g., in radial walls forming a Casparian strip) or suberin (e.g., in the walls of cells forming a suberin lamellae) (Enstone & Peterson, 2005; Von Wangenheim *et al.*, 2017) may obstruct "apoplastic" elements of water pathways around specific cell protoplasts. For brevity, a local element of water pathway will be referred to as apoplastic, symplastic or a transmembrane "pathway", depending on its nature. Pathways that connect the root surface to xylem vessels will be referred to as "radial pathways".

A major specificity of water flow principles across plasma membranes is membrane semi-permeability. Membranes exclude specific solutes, thus generating cell turgor through the principle of osmosis (Katchalsky & Curran, 1967). The impact of solute selectivity on water flow across a membrane is formulated via a "reflection coefficient" (σ, dimensionless). The coefficient typically ranges between one (which applies to water flowing through a perfectly

selective membrane) and zero (which applies to water flowing through a medium completely permeable to solute, e.g. cell primary wall and plasmodesmata), though negative values have been reported for strong basic anion exchange membranes (Pusch & Woermann, 1970). In case σ is null, the water pressure difference ($\Delta\psi_p$, MPa) alone drives the water flow. Otherwise, the osmotic potential difference ($\Delta\psi_o$, MPa) contributes as an additional driver in the water potential difference. Each piece of water pathway is also characterized by its hydraulic conductance (K, $m^3MPa^{-1}s^{-1}$) resulting from its pore size distribution and geometry. Because water flow across roots is laminar (the Reynolds number is orders of magnitude too low to generate turbulence at this scale, see Gunning (1976)), local water flow rates (Q, m^3s^{-1}) are proportional to the associated K. Using appropriate values for σ, the following general equation describes water flow through plasmodesmata, membranes, and walls at the sub-cellular scale:

$$Q = K (\Delta\psi_p + \sigma \Delta\psi_o) \quad (1)$$

Different approaches are used to estimate the intrinsic conductivities of each of the three types of pathway. Firstly, plasma membrane hydraulic conductivity (i.e. conductance per membrane surface unit, L_p) is the most accessible of these properties. It can be measured with a cell pressure probe (Steudle & Jeschke, 1983). The foremost contribution of aquaporins to L_p can be quantified by repeating the measurement after acid loading, which provokes the closure of aquaporins due to their protonation (Tournaire-Roux *et al.*, 2003). Secondly, the hydraulic conductance of individual plasmodesmata (K_{PD}) cannot be measured experimentally with the techniques currently available. However, their aperture can be estimated from the permeability of plasmodesmata to dyes (e.g., Lee *et al.*, 2011). Recent studies still estimate K_{PD} with the Poiseuille-Hagen law (e.g., Foster & Miklavcic, 2017), and account for the partial occlusion of plasmodesmata by a desmotubular structure, leaving water pathways that are only one order of magnitude wider ($2\ 10^{-9}$ m) than the aperture of an aquaporin (Terry & Robards, 1987; Tornroth-Horsefield *et al.*, 2006). Then, scaling K_{PD} to the cell level requires data on plasmodesmata frequency (Ma and Peterson 2001). Thirdly, estimations of the hydraulic conductivity of cellulosic walls (i.e. conductance per ratio of wall cross-section to wall length, k_w) remain highly uncertain, with reported values spreading over three orders of magnitude (Steudle and Boyer, 1985; Zhu & Steudle, 1991).

Our understanding of the quantitative impact of cell walls, aquaporins, and plasmodesmata on root radial permeability is hindered by their highly organised distribution in the root hydraulic network. However, according to Fiscus and Kramer (1975), capturing this level of complexity is not necessary to predict the bulk radial flow of water. One may simply represent the root as a single semi-permeable membrane:

$$J_w = k_r (\psi_{p,s} - \psi_{p,x} + \sigma_r (\psi_{o,s} - \psi_{o,x})) \quad (2)$$

where J_w is the water flux at the root surface ($m^3\ m^{-2}\ s^{-1}$), k_r is the root radial conductivity ($m^3\ m^{-2}\ s^{-1}\ MPa^{-1}$, note that here conductivity stands for conductance per root surface area), $\psi_{p,s}$ and $\psi_{p,x}$ correspond to the water pressure potential at the root surface and in xylem vessels, respectively, relative to the atmospheric pressure (MPa), σ_r is the effective root reflection coefficient (dimensionless, not to be confused with the reflection coefficient of a cell membrane), and $\psi_{o,s}$ and $\psi_{o,x}$ correspond to the osmotic potential at the root surface and xylem vessels, respectively (MPa).

Equation 2 is an effective equation as it merges indirectly root anatomical and cell-scale hydraulic properties into simple effective parameters (k_r and σ_r). Whether or not this equation remains accurate for any combination of hydraulic properties, anatomy and environment is still unclear. Remarkably, k_r values measured with the root pressure probe (Steudle & Jeschke, 1983) by varying the xylem pressure potential (i.e. "hydrostatic experiment", either as a pulse followed by pressure relaxation, or as a steady-state pressure clamp) systematically differ from values measured by varying the osmotic potential of the root bathing solution (i.e. "osmotic experiment") (Steudle & Frensch, 1989). Two main hypotheses have been proposed to explain such k_r differences. First, water flow across the semi-permeable endodermis generates the accumulation of solutes on the upstream side of the endodermis. This so-called "sweep-away effect" results in a bias in the estimated osmotic component of water potential, though it would not have time to form in the short pressure relaxation experiments (Knipfer et al., 2007). Due to the small volume of water involved and transient nature of the experiment, the pressure relaxation method might however suffer from interferences with the capacitance of the system, leading to an overestimation of k_r (Bramley *et al.*, 2007). The second hypothesis is that the water-filling of intercellular spaces in hydrostatic experiments may offer an increased area with low friction for radial water flow (Steudle & Peterson, 1998), resulting in a more conductive apoplastic

radial pathway from the root surface to xylem vessels. In order to account for the separate contributions of purely apoplastic and other parallel radial pathways ("cell-to-cell"), Steudle and Boyer (1985) propose calculating k_r as the average of cell wall and membrane conductivities weighted by their respective transverse surfaces. A similar approach has been used to determine the parameter σ_r of eq. (2) for the "composite transport model" (Steudle & Frensch, 1989).

Though widely accepted, this simple model of radial water flow fails to explain several experimental results. For instance, cortex cell L_p may not correlate with k_r (Hachez *et al.*, 2012), in contradiction with predictions of the composite transport model. Furthermore, the mere possibility of a substantial purely apoplastic radial pathway has recently been questioned (Knipfer & Fricke, 2010). Approaches combining experiments and functional-structural models constitute an asset to understand such complex systems (Band *et al.*, 2014; Postma *et al.*, 2017), so that a consistent framework from the cell to the root scale has become central to investigate questions of root radial transport. A two-dimensional radial-axial version of such a framework has recently been proposed by Foster and Miklavcic (2016; 2017) to investigate the role of apoplastic barriers in the salt stress response of Arabidopsis (*Arabidopsis thaliana*) roots. Addressing the complexity of radially asymmetric anatomical features in water transport questions would, however, necessitate the development of a complementary tool.

In this study, we developed a two-dimensional transverse model of the root hydraulic anatomy (MECHA) built on the scientific community's understanding of cell hydraulics. The model is meant to address questions pertaining to the impact of root anatomy and sub-cellular hydraulics on water transport in the transverse plane. Its insight may however be extended to three-dimensional root segments as long as their anatomy, hydraulic properties, and environment do not vary substantially in the longitudinal direction.

In the following, we firstly introduce the model. Secondly, we conduct a meta-analysis comparing maize (*Zea mays*) k_r experimental values reported in the literature to predictions of MECHA using anatomical and sub-cellular hydraulic data from the literature. Thirdly, through simulations of pressure clamp and osmotic experiments, we investigate whether the observed differences in k_r might arise from the water-filling of intercellular spaces or from

the solute sweep-away effect of apoplastic barriers. Finally, we estimate the contribution of plasmodesmatal conductance and L_p to root k_r, with a focus on specific tissues.

Results

Overview of the new model of transverse root water flow

Information on root anatomy and cell hydraulics were combined to build a finite difference model (MECHA) explicitly solving the equations of steady-state water flow (eq. (1) and Notes S1) across the network of individual cells. The model accommodates several plant species and root types, as shown in our Shiny application (https://plantmodelling.shinyapps.io/mecha/) for Arabidopsis and pearl millet (*Pennisetum glaucum*). Here we report the case of maize.

From the anatomical perspective, the model uses cell geometry and connectivity information collected from a cross-section image of the primary root of maize (Figure 1a) and vectorized with the CellSet program (Pound *et al.*, 2012) (Figure 1c). From the hydraulic perspective, the information includes maize literature data (Figure 1b, Tables 1 and 2) of cell primary wall hydraulic conductivity (k_w, which is an intrinsic conductivity in units of $m^2\ s^{-1}\ MPa^{-1}$), cell plasma membrane permeability (L_p, $m\ s^{-1}\ MPa^{-1}$), hydraulic conductance of individual plasmodesmata (K_{PD}, $m^3\ s^{-1}\ MPa^{-1}$), their frequency in each root tissue, and membrane reflection coefficients (σ, dimensionless). These conductivities are combined in a scheme analogue to electric circuits (Figure 1d) over the root anatomical layout to constitute the explicit root hydraulic anatomy (Figure 1e).

The model simulates solute radial convection-diffusion in the apoplast at steady state (solute diffusivity parameter in Table 2). According to pressure clamp experiments and modelling analyses (Knipfer et al., 2007), the solute distribution reaches such a steady-state within a few seconds of alterations of the water flow rate. Because the focus of the present study is on water flow, we assumed solute homeostasis in the symplast and solved solute transport only in the apoplast. The assumption of symplastic homeostasis does not exclude the transfer of major solutes through plasmodesmata with the mass flow of water. Solutes leaving the protoplast symplastically may indeed largely be replaced by the transmembrane transport at rates reported in the literature (Notes S2).

The computation of flow equations in the transverse hydraulic network yields steady-state water flow rates across each individual piece of the hydraulic pathways (Figure 1f, and Notes S3) and the hydrostatic water pressure in cell walls and protoplasts. Furthermore, effective metrics such as root k_r and σ_r are extracted from the simulations (Figure 1g).

Experimental k_r values are best predicted using high values of k_w and low values of K_{PD} from the literature

MECHA parameterized with experimental cell-scale hydraulic properties (Table 2) yielded radial conductivities that fall in the range of measured maize root k_r (measurements: coloured boxes in Figure 2a; simulations: symbols with legend from Figure 2b, water-permeable and impermeable apoplastic barriers in grey and black, respectively).

The combination of high cell k_w and low K_{PD} generated the best match with the experimental range of young maize root k_r and reproduced qualitatively the longitudinal trend estimated by Doussan *et al.* (1998b) (Figure 2a). A systematic mapping of the "L_p - k_w - K_{PD}" parametric space with 10^3 sets of parameter values confirmed that this parametrization is in the direct vicinity of the overall best fit (Notes S4).

When increasing the water-permeability of lignified and suberized cell walls from zero to their upper possible limit (Table 2), k_r increased by 36% ± 46% (n=12, maximum +136%, see black versus grey symbols in Figure 2a) and σ_r decreased from 1 to 0.88 ± 0.05 (n=12, minimum 0.79, see Figure 2b). Furthermore, the predicted fraction of fully apoplastic radial flow went from 0 to 9.9% ± 5.5% (n=12, maximum 21%) and was highly negatively correlated to σ_r (r= -0.98, see dataset S1).

The impact of aquaporin gating (reducing k_{AQP} by 95%) on k_r was less pronounced in the case of low k_w (-37% ± 3%, n=12, minimum -45%) than high k_w (-57% ± 9%, n=12, minimum -74%). The latter is closer to values of -60% to -70% reported experimentally (Ye & Steudle, 2006; Boursiac *et al.*, 2008; Parent *et al.*, 2009).

The simulations also confirmed the limited impact of the geometrical positioning of transverse cell walls on k_r. On the one hand, hydraulic anatomies "A" with aligned transversal cell walls overestimated the value of k_r as compared to more realistic non-

aligned systems “B” that had longer apoplastic pathways. On the other hand, the latter system had higher k_r than a system “C” with obstructed transversal walls. Considering that in our results the difference between k_r values in systems “A” and “C” was always less than 2.5% (see dataset S2), we conclude that the difference between k_r values in systems “A” and “B” may not be substantial.

The water-filling of cortex intercellular spaces may not be responsible for experimental differences between osmotic and hydrostatic k_r

The relative difference between k_r in hydraulic anatomies with air- and water-filled intercellular spaces (representative of hydrostatic and osmotic experiments, respectively) was only 1.3% ± 0.1% under high k_w (n=12, maximum 2.8%), including scenarios with water-permeable apoplastic barriers, and 92% ± 6% under low k_w (n=12, maximum 158%, see dataset S1). This impact is lower than hypothesized by Steudle and Peterson (1998), even though we intentionally overestimated k_r in case of water-filled intercellular spaces to obtain an upper possible bound.

The Casparian strip solute sweep-away effect biases the estimation of k_r in osmotic experiments more than in pressure clamp experiments

In conditions of perfect mixing of apoplastic solutes (i.e. infinite apoplastic solute diffusivity), the simulated fluxes yielded unique k_r and σ_r, regardless of xylem pressure and bathing solution osmotic potential. In consequence, the “water flux vs. $\Delta\psi$” relation was linear (e.g., thick black lines in Figure 3b,d) in compliance with the model of the root as a semi-permeable membrane (eq. 2, Fiscus and Kramer (1975)).

When assuming finite solute diffusivity, apoplastic solute convection-diffusion affected the estimation of k_r in virtual pressure probe experiments. We first investigated the case of the hydraulic anatomy with high k_w and low K_{PD}. In virtual pressure clamp experiments with increasing pressure clamps, the outward water flow provoked the accumulation of solutes on the stele side of the endodermis and their depletion on the cortex side (Figure 3a, light and darkest blue for xylem pressure increased by 0.025 and 0.125 MPa, respectively). These alterations of the osmotic potential partly countered the outward driving pressure of water, thus reducing the absolute radial flow rates (light to dark blue dots in Figure 3b) as

compared to the case of perfect solute mixing (black dots in Figure 3b). Because the water potentials at the root surface and in the xylem vessels are used in the estimation of k_r (eq. 3, Methods) instead of the full profile of water potentials, the driving force of water flow was overestimated and k_r underestimated by a factor 1.2 to 1.6 (for higher and lower limits of solute diffusivity, respectively). Another consequence was that the "water flux vs. $\Delta\psi$" relationship, the slope of which corresponds to k_r, became slightly nonlinear. These features were exacerbated in the osmotic experiment (Figure 3c), in which k_r was underestimated by a factor 2.7 to 7.5 (Figure 3d).

It is particularly interesting that, for a hydraulic anatomy with low k_w (Table 2), k_r values estimated in the same experiments were barely underestimated and did not differ substantially between pressure clamp and osmotic experiments. The biases reached 1.02 to 1.08 and 1.1 to 1.3 in pressure clamp and osmotic experiments, respectively.

In Notes S5 we demonstrate that our results were not affected by spatial variations of osmotic potential in the symplast.

Endodermis L_p and plasmodesmatal conductance are the most limiting elements of water pathway before and after the suberization of the endodermis, respectively

In the distal region of the root that has an endodermal Casparian strip but no suberized walls, the impact of the plasma membrane hydraulic conductivity (L_p) on k_r peaked in the scenario with high k_w and low K_{PD}. The increase of k_r per unit increase of L_p (hereafter referred to as "sensitivity", eq. 6, Methods) was 72% (see slope of the dark blue curve in Figure 4g). This value is particularly high, considering that the sum of sensitivities to all individual pieces of pathways (also including plasmodesmata and cell walls) sums up to 100% by definition. Furthermore, the endodermis L_p alone accounted for 69% of the overall sensitivity (Figure 4h). In other words, the permeability of endodermis plasma membranes was the bottleneck controlling k_r except when endodermal suberization was complete (Figure 4b).

As a matter of comparison, the cortex L_p accounted for less than 1% of the overall sensitivity (i.e. k_r was essentially independent from cortex L_p, Figure 4h). The latter independence may explain the absence of correlation between k_r and cortex L_p reported in the literature

289 (Hachez et al., 2012). The systematic exploration of the parametric space revealed that such
290 a low sensitivity to cortex L_p occurs when the composite nature of the root allows the bypass
291 of cortex membranes by flowing across the cortex either along the apoplastic or the
292 symplastic pathway. This symplastic bypass occurred when low k_w and high K_{PD} were
293 combined (Notes S4), with 51% of the overall sensitivity controlled by K_{PD}. Conversely, if
294 both k_w and K_{PD} were low, water would not bypass cortex membranes, and k_r would be
295 systematically be more sensitive to cortex L_p than to endodermis L_p (Figure 4c,f,i).

296 The sensitivity of k_r to plasmodesmatal conductance evolved with the maturation of
297 apoplastic barriers in the scenario with high k_w and low K_{PD}. It was as high as 23% before
298 endodermal suberization (cyan curve in Figure 4g), and reached 73% at maturity (cyan curve
299 in Figure 4a), thus becoming the new bottleneck for radial water flow. As a matter of
300 comparison, the sensitivity of k_r to k_w was lower than 5% in this scenario.

301 ## Discussion

302 **Models of water flow across root tissues are not functionally equivalent**

303 Models of water flow across root tissues (see overview of major approaches in Figure 5)
304 have been elaborated with the purpose of addressing specific scientific questions. In the
305 composite transport model (Steudle and Boyer, 1985; Steudle and Frensch, 1989), water
306 flow is partitioned between two parallel radial pathways (apoplastic versus cell-to-cell), each
307 with specific conductivities and reflection coefficients. This simple representation assumes
308 uniform cell properties and no substantial variations of osmotic potential in each root
309 compartment. However, its major interest lies in the generalisation of eq. (2), explicitly
310 separating apoplastic and cell-to-cell pathways while being compatible with root system
311 scale hydraulic models (e.g. Doussan et al., 1998a).

312 The two-dimensional discretisation of the root tissue hydraulic network proposed by
313 Zwieniecki et al. (2002) allowed analysing the impact of radial and longitudinal variations of
314 tissue properties on water flow across roots. It was lately completed by Foster and Miklavcic
315 (2017) who separated apoplastic and symplastic domains at the cell scale in order to
316 precisely address interactions between the transport of major solutes (K^+, Na^+, H^+, Cl^-) and
317 water flow across cell walls, membranes and plasmodesmata.

The MECHA model relaxes the constraint of radial symmetry present in all previous models by allocating two spatial dimensions to the transverse domain, thereby allowing the proper inclusion of complex anatomical features (e.g., xylem poles, passage cells, etc.) and a more realistic description of root anatomy from microscopic images. Unlike Foster and Miklavcic (2017), the sub-cellular discretisation accommodates the presence of intercellular spaces, variations of water pressure along the walls of the same cell, and the localization of Casparian strips in radial walls. The current version of MECHA is suitable to address questions of water flow in root segments with little variation along the longitudinal axis in terms of hydraulic properties (e.g., distal differentiated 10 cm of maize roots grown in hydroponics, excluding the elongation zone) and in terms of environment (e.g., root in a bathing solution), as in the root pressure probe experiments simulated in this study. Longitudinal variations of hydraulic properties or root environment might be accounted for by coupling MECHA with a one-dimensional root architectural model such as Meunier et al. (2017c).

Hydraulic properties are not always transferable between cell and root scales

The root radial hydraulic conductivity (k_r) has frequently been measured on the distal portion of maize primary roots (up to 14 cm long) using a root pressure probe. Data from Steudle *et al.* (1987), Zhu and Steudle (1991), Frensch and Steudle (1989), and Bramley *et al.* (2007) cover one order of magnitude but mostly meet around 2 10^{-7} m $s^{-1}MPa^{-1}$ (see coloured areas in Figure 2a). Similar data in mature root zones are rare, likely due to the presence of lateral roots that complicate the attachment of the probe. Doussan *et al.* (1998b) estimated a whole profile of root k_r along the maturation gradient by combining inverse modelling and cumulative flow data from Varney and Canny (1993) (see dashed line in Figure 2a, with the endodermal suberization between 15 and 19 cm from the tip and exodermis development between 45 and 60 cm from the tip). The similarity between k_r measured and predicted from the cell scale strengthens the hydraulic anatomy approach, particularly when considering that the experimental k_r range for maize (overall 2 10^{-8} to 3 10^{-7} m $s^{-1}MPa^{-1}$, see boxes in Figure 2a) appears relatively narrow in view of values reported in the literature for other plants. For instance, McElrone *et al.* (2007) measured k_r values from 10^{-5} to 10^{-4} m $s^{-1}MPa^{-1}$ with an ultra-low flowmeter in deep fine roots of live oak (*Quercus*

fusiformis) and Gum Bumelia (*Sideroxylon lanuginosa*), while Zarebanadkouki *et al.* (2016) obtained k_r values of 10^{-6} m $s^{-1}MPa^{-1}$ in undisturbed white lupine (*Lupinus albus*) primary roots by combining deuterium tracing, inverse modelling, and analytical hydraulic functions developed by Meunier *et al.* (2017a).

Our results support the simplification of the "root as a semi-permeable membrane", which perfectly captures the process of transverse water flow in absence of variations of osmotic potential within the symplast and apoplastic domains. It also captures it reasonably well when these variations are small (Figure 3a,b), thereby allowing the transfer of hydraulic properties from the cell to the root scale. However, in particular conditions (e.g. osmotic experiments), the solute sweep-away effect due to the Casparian strip may generate a substantially nonlinear response of water flow to water potential difference between root surface and xylem vessels (Figure 3c,d), so that eq. (2) (Fiscus & Kramer, 1975) is no longer accurate. Water flow models are generally not fully compatible across scales, as found in root water uptake models (Feddes et al., 1978; Javaux et al., 2013; Couvreur et al., 2014), or in hydrological models (Pokhrel & Gupta, 2010; Brynjarsdóttir & O'Hagan, 2014; Couvreur et al., 2016), which is reason for introducing effective principles. Key structures or processes (e.g. solute diffusion-convection) too complex to be represented with simple physical equations at larger scale may explain such incompatibilities. An effective "osmotic k_r" might thus inform reasonably well on expected water flow rates in conditions similar to the osmotic experiment, while being disconnected from actual cell scale hydraulic properties.

The estimation of k_r is more biased in osmotic experiments due to a solute sweep-away effect than in hydrostatic experiments due to the water-filling of intercellular spaces

In this study, we report changes of k_r between hydraulic anatomies with air-filled *vs* water-filled intercellular spaces that are by far lower than one order of magnitude. This suggests that the intercellular space water-filling hypothesis proposed by Steudle and Peterson (1998) may not explain the ten-fold increase of k_r between osmotic and hydrostatic experiments (Steudle *et al.*, 1987; Steudle & Frensch, 1989). Despite their high hydraulic conductivity and simulated three-dimensional connectivity when water-filled, intercellular spaces are in series with less conductive pieces of pathway that limit variations of k_r (e.g., at the endodermis, even when the Casparian strip is water-permeable). Note that this interpretation applies to

root regions that developed at least a Casparian strip, and thus does not deny interpretations on the dominant role of intercellular spaces in water flow across slices of potato (*Solanum tuberosum*) storage organs (Michael et al., 1997).

The hydraulic anatomy approach therefore suggests that features other than water-filled intercellular spaces likely generated the systematic differences between k_r measured in osmotic and hydrostatic experiments. In this study, we hypothesize, and support with simulations, that most of the reported k_r differences between pressure clamp and osmotic experiments may stem from the erroneous estimation of the osmotic driving pressure (Figure 3c,d), as argued by Knipfer and Fricke (2010). Substantial biases in the estimation of k_r (factor 2.7 to 7.5) were simulated when the majority of the transmembrane flow was located near the Casparian strip, i.e. for parameter sets with high cell wall hydraulic conductivity (k_w). Interestingly, this bias did not appear in our simulations when using low k_w, which may be a critical property explaining that hydrostatic and osmotic k_r do not differ in wheat (*Triticum aestivum*) (Bramley *et al.*, 2007).

While the biased estimation of maize k_r in osmotic experiments is likely, it may be combined with actual alterations of the root radial conductivity, for instance due to changing cell L_p in response to osmotic stress. However, while a decrease of L_p may entail a reduction of k_r in an osmotic experiment, the literature reports increasing L_p with decreasing root medium water potential (from -0.075 to -0.34 MPa, Hachez *et al.* (2012)). Plasmodesmatal aperture also responds to the root osmotic environment (Roberts & Oparka, 2003), but quantitative data is lacking so far.

Simulation results suggest testing whether endodermis L_p or plasmodesmatal conductance vary with k_r in response to osmotic stress

The experimental observation that maize cortex L_p varies independently of the hydrostatic k_r (Hachez *et al.*, 2012) was reproduced in our simulations whenever the water stream bypassed cortex membranes via the apoplast (for combined high k_w and low K_{PD}) or via the symplast (for combined low k_w and high K_{PD}). In the former case, 69% of the variability of k_r was controlled by the endodermis L_p, while in the latter case plasmodesmatal conductance controlled 51% of variability. Identifying which property (endodermis L_p or K_{PD}) varies in

coordination with k_r before and after osmotic stress may thus indicate whether the bypass of cortex plasma membranes is apoplastic or symplastic. These hypotheses could be tested indirectly by using immunocytochemistry to quantify *Zea mays* plasma membrane intrinsic protein (ZmPIP, aquaporin) expression in the endodermis (Hachez *et al.*, 2006) and callose distribution across the root (Baluška *et al.*, 1999).

While the modelling approach alone could not explain the precise reason why maize cortex L_p varies independently of the hydrostatic k_r, it may narrow the number of hypotheses down to the few ones compatible with the physics of water flow. This inexpensive mathematical tool needs to be integrated in an iterative loop combining experimental and modelling approaches to express its full potential.

High cell wall hydraulic conductivity values are necessary to reproduce four root responses reported experimentally

Estimated values of cell primary wall hydraulic conductivity (k_w) reported in the literature vary by orders of magnitude. In this study, most illustrations depict root properties resulting from either "low" k_w value estimated by Tyree (1968) and "high" k_w values measured by Steudle and Boyer (1985) (three orders of magnitude apart) and are completed by systematic investigations of the multidimensional parametric space spanning six orders of magnitude. While this parameter is hardly measurable, the modelling approach demonstrated that the value of k_w needs to be high in order to reproduce four types of experimental observations.

Firstly, high k_w was necessary to generate the significant longitudinal variations of k_r (stars and closed circles in Figure 2a) assumed to result from apoplastic barrier deposition (Sanderson, 1983; Doussan *et al.*, 1998b; Barrowclough *et al.*, 2000). Such observed changes could also be the result of longitudinal differences in cell membrane properties, but this is unlikely as differentiated cell L_p was reported to be longitudinally uniform in maize and onion (*Allium cepa*) (Barrowclough *et al.*, 2000; Zimmermann *et al.*, 2000).

Secondly, the simulated response of k_r to the gating of aquaporins was close to changes observed experimentally (Ye & Steudle, 2006; Boursiac *et al.*, 2008; Parent *et al.*, 2009), with the condition that the value of k_w in the parameter set was high.

Thirdly, effective k_r values obtained from simulated osmotic and pressure clamp experiments only differed significantly in the case of high k_w, reproducing the observation of effectively different osmotic and hydrostatic k_r (Steudle *et al.*, 1987).

Finally, high k_w was also necessary to reproduce the absence of correlation between cortex L_p and k_r reported experimentally (Hachez *et al.*, 2012), except when the plasmodesmatal conductance was high.

Conclusion

MECHA is a hydraulic model which computes the flow of water through the walls, membranes, and plasmodesmata of each individual cell throughout a complete root cross-section. From this fine scale, the model predicts root reflection coefficient (σ_r) and radial permeability (k_r) for the root cylinder approach used in plant scale models. Hence it connects hydraulic theories across scales based on detailed anatomical descriptions and experimental data on the permeability of cell walls (k_w), membranes (L_p), and plasmodesmata (K_{PD}). Its two transverse spatial dimensions allows accounting for radially asymmetric features, such as intercellular spaces and the location of xylem poles or passage cells, on water flow rates across the root.

Using the anatomical structure of a maize root with cell hydraulic properties from the literature, MECHA simulated root k_r values that fit the range of measurements from the literature and the k_r response to aquaporin gating. In particular, a relatively high cell k_w (Steudle & Boyer, 1985) and low K_{PD} (Bret-Harte & Silk, 1994) yielded the best fit. The water-filling of intercellular spaces did not affect k_r enough to explain the ten-fold difference between k_r estimations in hydrostatic and osmotic experiments, unlike hypothesized by Steudle and Peterson (1998), but variations of the osmotic potential in radial walls, not accounted for in root radial flow models, might explain a major part of these differences. In case of high cell k_w, the simulated root k_r did not correlate with cortex cell L_p, as observed experimentally (Hachez *et al.*, 2012). The model also suggested that root k_r might be very sensitive to the aperture of plasmodesmata, despite their low conductance.

The proposed enrichment of the composite transport model sheds new light on the field of plant water relations. Cutting-edge research on hydropatterning (Bao et al., 2014),

hydrotropism (Dietrich et al., 2017), and apoplastic barriers (Barberon et al., 2016; Doblas et al., 2017) recently highlighted the need for a quantitative hydraulic framework to address questions related to pressure distribution and water flow direction at the cell scale. The model compatibility with a root anatomical software (Pound et al., 2012) and functional-structural-plant-models (Javaux et al., 2008) may open avenues to investigate the relationships between root architecture, anatomy, and water availability.

Future developments of the model will focus on the integration of an explicit third spatial dimension, as proposed in a simpler scheme by Zwieniecki *et al.* (2002), to investigate axial variations of water pressure and flow along roots. While MECHA can be used with the roots of virtually any plant species, as illustrated in the online visualisation interface (http://plantmodelling.shinyapps.io/mecha) with Arabidopsis and pearl millet, the collection of cell hydraulic data for these species is a future challenge. The methods used by (Hachez *et al.*, 2012) in maize could presumably be transferred to other plants with no major issue. Furthermore, recently developed techniques, such as serial block face scanning, offer great potential to estimate plasmodesmata frequency throughout organs (Ross-Eliott *et al.*, 2017). Finally, with the proposed modelling approach, we offer possibilities to estimate cell hydraulic properties by inverse methods as illustrated in this study.

Methods

Cell level hydraulic parametrization

While illustrations provided in this study focus on a limited number of "default", "high" and "low" parameter values from the literature, a wide range of cell hydraulic parameter values (10^3 triples in the "L_p - k_w - K_{PD}" parametric space) were tested in order to finely explore the impact of parametrization on responses of the maize (*Zea mays*) root hydraulic anatomy.

The hydraulic conductance of individual plasmodesmata (K_{PD}) was evaluated from their geometry by Bret-Harte and Silk (1994) in maize, accounting for its partial occlusion by the desmotubule and increased viscosity of water in channels at the nanometre scale (3.4 mPa s). The obtained K_{PD} values ranged from 3.05 10^{-19} to 1.22 10^{-18} $m^3s^{-1}MPa^{-1}$ (geometrical average: 6.1 10^{-19} $m^3s^{-1}MPa^{-1}$, here referred to as "low K_{PD}"). Their estimation was an order of magnitude less than estimated by Ginsburg and Ginzburg (1970) in maize (3.54 10^{-18} m^3s^{-}

^{1}MPa^{-1}, here referred to as "high K_{PD}"), assuming a plasmodesmata frequency of 0.48 µm^{-2} (Ma and Peterson, 2001) to turn the conductivity into a conductance per plasmodesmata. For the systematic exploration of the parametric space, we used 10 K_{PD} values ranging from 7.2 10^{-20} to 3.7 10^{-17} m^{3}s^{-1}MPa^{-1}.

Plasmodesmatal conductances were scaled to the cell level through multiplications by plasmodesmata frequency (µm^{-2}) and shared wall surface (µm^{2}) of neighbouring cells. Plasmodesmata frequency data in maize roots after cell elongation were obtained from Warmbrodt (1985) and Clarkson *et al.* (1987) (reported by Ma and Peterson (2001), see Table 1). Shared wall surface estimations were based on the discretised root cross-section anatomy for 200-µm-long cells. An effective plasmodesmatal conductivity per membrane surface area (k_{PD}) of 2.4 10^{-7} m s^{-1}MPa^{-1} was estimated from the low K_{PD} and average plasmodesmata frequency (0.4 µm^{-2}).

The default cell L_p value was obtained from the cell pressure probe estimation of Ehlert *et al.* (2009) (5.3 10^{-7} m s^{-1}MPa^{-1} after removal of k_{PD}). From the reported difference between hydraulic conductivities of control and acid load treatments, the contributions of aquaporins (k_{AQP}) and the phospholipid bilayer (k_m) were estimated as 5.0 10^{-7} m s^{-1}MPa^{-1} and 2.6 10^{-8} m s^{-1}MPa^{-1}, respectively. For the systematic exploration of the parametric space, 10 k_{AQP} values were used ranging from 1.4 10^{-8} to 7.4 10^{-6} m s^{-1}MPa^{-1}.

Pressure probe estimations of cellulosic wall hydraulic conductivity were taken from Steudle and Boyer (1985), who measured in soybean (*Glycine max*) a value of 7.7 10^{-8} m^{2}s^{-1}MPa^{-1} (here referred to as "high k_w") and Tyree (1968) who reported a value of 1.4 10^{-10} m^{2}s^{-1}MPa^{-1} in Nitella (*Nitella flexilis*) (here referred to as "low k_w"). Note that Zhu & Steudle (1991) observed intermediate values of 2.5 10^{-10} to 6.1 10^{-9} m^{2}s^{-1}MPa^{-1} in maize. For the systematic exploration of the parametric space, 10 k_w values were used ranging from 1.8 10^{-13} to 1.4 10^{-7} m^{2}s^{-1}MPa^{-1}.

The hydrophobic Casparian strips and suberin lamellae were attributed null hydraulic conductivities, except in scenarios investigating the hypothesis of water-permeable apoplastic barriers. In this case, from the Poiseuille-Hagen law, the hydraulic conductivity of

lignified cell walls, whose pores are 1 nanometre wide (Deng *et al.*, 2016), was estimated as no more than 10^{-11} $m^2 s^{-1} MPa^{-1}$, which was used as "leaky" upper limit.

As plasmodesmata and primary cell walls are not selective for cell solutes, they were attributed null σ. For simplicity, membranes were assumed to be fully selective (σ = 1), which is particularly representative of experiments using mannitol (Fritz & Ehwald, 2011). Finally, the bulk solute diffusivity value in cell walls (4 10^{-11} m^2 s^{-1}) was obtained from Knipfer et al. (2007) experimental estimations. A summary of cell scale hydraulic properties is displayed in Table 2.

Cross-section geometry and cell typology

The hydraulic network geometry reproduced the anatomy of an aeroponically grown maize primary root (0.9 mm diameter), five centimeters proximal to the tip. A cross-section stained by immunocytochemistry for the cellular distribution of ZmPIP2;1 and ZmPIP2;2, two plasma membrane aquaporins, was observed with an epifluorescent Leica DMR microscope (Wetzlar, Germany) as in Hachez *et al.* (2006). The captured image was segmented with the program CellSet (Pound *et al.*, 2012) and individual cells and structures were labelled manually (xylem, epidermis, exodermis, cortex, endodermis, pericycle, and stele parenchyma) based on their shape and position in the cross-section (Figure 6a). Phloem elements and their companion cells could not be identified at that resolution. However, as they do not bear apoplastic barriers and represent a relatively small fraction of the cross-section, we assumed that their specific properties did not significantly impact root k_r and labelled them as their neighbour stele parenchyma cells. Cortex intercellular spaces (204 in total in this cross-section) were recognized based on their relatively small size as compared to the surrounding cells.

Three stages of apoplastic barrier development in the transverse plane (structured deposition of hydrophobic material in cell walls) were selected for this study: (i) presence of Casparian bands between endodermis cells, (ii) presence of suberin lamellae covering the endodermis, except for three passage cells located in front of early metaxylem vessels, and (iii) presence of suberin lamellae covering the whole endodermis combined with an exodermal Casparian strip (see null apoplastic fluxes in both apoplastic barriers in Figure 6b).

To isolate the impact of apoplastic barrier deposition on root k_r and water pathways, the same network geometry was used for all simulations, and cell wall hydraulic properties were adjusted at apoplastic barrier locations.

The cross-section was given a pseudo three-dimensional representation by attributing a height of 200 µm (the typical length of maize elongated root cells) to the system. Transverse cell walls were thus included on top and at the bottom of the cross-section. In consequence, the top and bottom of cells were aligned in our model.

Calculation of the theoretical root radial conductivity and reflection coefficient from the cell scale

The root radial conductivity k_r is defined as the root water uptake rate (Q_w, $m^3 s^{-1}$, positive inwards) per unit root surface under a unit pressure difference between root surface and xylem, where the pressure difference is $\psi_{p,s}$ - $\psi_{p,x}$ + σ_r ($\psi_{o,s} - \psi_{o,x}$) (Fiscus & Kramer, 1975). As σ_r was unknown at first, k_r was obtained by running MECHA (method for solving water flow equations detailed in Notes S1) under uniform osmotic potential throughout the cross-section for non-null pressure differences. Any pressure difference ($\psi_{p,s}$ - $\psi_{p,x}$) should in principle yield the same value of k_r, which was verified with the following equation for pressure differences of 0.025 to 0.125 MPa by increments of 0.025 MPa:

$$k_r = \frac{Q_w}{2\pi r h\left(\psi_{p,s} - \psi_{p,x} + \sigma_r\left(\psi_{o,s} - \psi_{o,x}\right)\right)} \quad (3)$$

Where r (m) is the root radius, h (m) the height of the cross-section, and osmotic potentials canceled out. Note that the variable Q_w was calculated by summing up water flow rates at the root surface.

The effective parameter σ_r was calculated by running MECHA under no-flow conditions with $\psi_{o,s}$ different from $\psi_{o,x}$ (see default boundary conditions in Table 3):

$$\sigma_r = \frac{\frac{Q_w}{2\pi r h k_r} - \psi_{p,s} + \psi_{p,x}}{\psi_{o,s} - \psi_{o,x}} \quad (4)$$

where Q_w was set to 0, and the xylem pressure at equilibrium was an output of the model. The model was also run for various osmotic potentials at the root surface in order to verify the unicity of σ_r (see "Various $\psi_{o,s}$" in Table 3) for known k_r and $\psi_{p,x}$ (Q_w then being an output of the model).

Note that in this section solutes were assumed to be perfectly mixed on either side of apoplastic barriers (i.e., the osmotic potential of all cell walls in the stele equals $\psi_{o,x}$, and the osmotic potential of all other walls equals $\psi_{o,s}$).

The comparison of simulated k_r with measured values from the literature was carried out for the 10^3 combinations of k_{AQP}, k_w and K_{PD} parameter sets reported in the section "cell level hydraulic parametrization" of the Methods. After comparing the overall ranges of measured and simulated values of k_r and σ_r, the cell hydraulic parameter set *P** that minimised the square differences with k_r from the literature was obtained. The combination of default, high or low cell hydraulic parameters (Table 2) that was closest to *P** was also identified.

Furthermore, statistics on the impact of (i) the maximum possible water-permeability of apoplastic barriers (Table 2), and (ii) the gating of aquaporins (k_{AQP} reduced by 95%), on k_r were evaluated for partitions of 24 parametric sets (i.e., combinations of high or low K_{PD}, high or low k_w, water-permeable or impermeable apoplastic barriers, and 3 stages of apoplastic barrier development). The cell parameter sets that best reproduced literature data on k_r response to aquaporin gating were identified.

Finally, whether the alignment of transverse walls in the virtual root provoked a significant overestimation of k_r, as compared to a more realistic tortuous apoplastic domain, was investigated. Root hydraulic anatomies with null transverse wall conductivities were used to estimate an upper bound to the difference between aligned and tortuous apoplastic domains.

Quantification of the impact of water-filling intercellular spaces on k_r

The root radial conductivity was calculated for hydraulic anatomies including air-filled intercellular spaces, then with water-filled intercellular spaces. In the hydraulic network, intercellular spaces were considered as pseudo-cells with particular properties: (i) K_{PD} was null (i.e. no plasmodesmata) and (ii) L_p depended on whether they were filled with air or water (i.e. mathematically allows the access to the centre of the intercellular space, or not).

If they were filled with air, there was no water pathway across the intercellular spaces, and L_p was set to zero (see blue intercellular polygons, i.e. null apoplastic fluxes, in Figure 6b). If they were filled with water, water may freely move from the cell wall to the centre of intercellular spaces, and L_p was set to infinity. In the water-filled case cortex cell wall hydraulic conductivities were also set to infinity to account for the possible three-dimensional connections between these spaces. In consequence, (i) all water-filled intercellular spaces were virtually connected, and (ii) the difference between k_r in the air- and water-filled cases was overestimated due to neglected frictions in the cortex apoplast in the water-filled case. This set an upper limit to the possible impact of water-filled intercellular spaces on the estimation of k_r in hydrostatic experiments.

The relative difference of k_r was characterized for all 24 combinations of apoplastic barrier development stages and cell hydraulic properties reported in Table 2.

Quantification of the impact of solute convection-diffusion on the estimation of k_r

An analytical solution of solute diffusion-convection in radial cell walls was implemented in MECHA to account for the feedback between solute distribution and water flow. Hydraulic anatomy with an impermeable endodermal Casparian strip, high k_w and low K_{PD} values (Table 2) was the main focus, which had fairly well conserved water velocities across the cortex and transmembrane flow concentrated in the direct vicinity of the endodermis. To a first approximation, the endodermis was considered a semi-permeable structure with unit reflection coefficient, as in Knipfer *et al.* (2007).

For a constant solute concentration at the root surface ($C(0)$, mOsmol per liter), full solute exclusion at the interface with endodermis membranes, and a uniform radial velocity of water in the cortex apoplast (u , m s^{-1}, positive inwards), the solution of solute distribution was:

$$C(r) = C(0)e^{\frac{-ur}{D}} \quad (5)$$

where r (m) is the radial position along the apoplast between the root surface (r = 0) and the endodermis, D (m^2 s^{-1}) is the solute diffusivity in the apoplast. Note that the radial velocity of water in the apoplast is obtained by dividing the simulated total radial flow rate (Q_w, m^3 s^{-1}) by the average radial cell wall cross-section area (m^2), which is very similar on either side of the endodermis. On the stele side of the endodermis, an analogous solution was used to

estimate solute diffusion-convection between xylem vessels and the surface of the endodermis.

Boundary conditions representative of exosmotic (i.e. water flowing from the stele toward root surface) pressure clamp and osmotic experiments were applied (Table 3), both starting with a bathing solution osmotic potential ($\psi_{o,s}$) of -0.02 MPa ("Johnson-solution") and a xylem pressure ($\psi_{p,x}$) at equilibrium ($P_{r\ 0}$, generating no water flow across the root). Cell cytosol and xylem osmotic potentials ($\psi_{o,c}$ and $\psi_{o,x}$, respectively) were set to the average values measured in maize cortex (-0.7 MPa) and xylem vessels (-0.15 MPa) by Enns *et al.* (2000). For the pressure clamp experiments, $\psi_{p,x}$ was sequentially increased by steps of 0.025 MPa up to a total of $P_{r\ 0}$ + 0.125 MPa. In osmotic gradient experiments, decreasing bathing solution osmotic potentials were applied by steps of -0.025 MPa, down to -0.145 MPa (i.e. Johnson-solution + 50 mOsM mannitol, using Van't Hoff's law to convert solute concentrations into osmotic potentials and vice versa). To offer a direct point of comparison with the pressure clamp experiment, the xylem pressure was maintained constant in this second type of experiment. Note that the current version of the model should not be used to simulate hydrostatic pressure relaxation experiments due to the steady-state flow assumption.

Because the water flux and solute distribution simultaneously affected each other, the problems of water flow and solute distribution needed to be solved iteratively until convergence, starting from uniform solute concentrations on either side of the endodermis. After convergence, k_r was calculated with eq. (3), and the relative bias was compared to the perfect mixing case.

To evaluate the sensitivity of the results to the selected value of solute diffusivity, the osmotic and pressure clamp virtual experiments were run with values of diffusivity divided or multiplied by 2 as compared to the default value estimated experimentally by Knipfer *et al.* (2007) (4 10^{-11} m^2 s^{-1}).

Finally, the same virtual experiments were repeated on a hydraulic anatomy with low k_w (Table 2) to investigate the impact of cell wall hydraulic properties on the generality of the results.

664 **Sensitivity analysis of root k_r to cell hydraulic properties**

665 The sensitivity (L_s, %) of root k_r to cell scale properties was quantified as the ratio of two
666 quantities: (i) the relative change of k_r (i.e. $\frac{\delta k_r}{k_r}$) resulting from a 1% change in a cell-scale
667 hydraulic property (e.g., L_p or K_{PD}), and (ii) the relative change of the latter cell scale
668 property denoted L (i.e. $\frac{\delta L}{L}$, here equal to 1.01), in percent units:

669 $$L_s = 100 \frac{\delta k_r}{\delta L} \frac{L}{k_r} \quad (6)$$

670 By definition, the sensitivity cannot exceed 100% (1:1 ratio). Furthermore, it can be
671 demonstrated that the sensitivities of k_r to non-overlapping elements of the hydraulic
672 network must be comprised between 0 and 100% and sum up to 100% when exhaustive.

673 On the one hand, a sensitivity analysis of k_r to an extensive list of cell scale properties (K_{PD}
674 and tissue specific L_p) was conducted for a limited number of hydraulic anatomies (three
675 stages of maturation of impermeable apoplastic barriers, low K_{PD}, and high or low k_w). On
676 the other hand, a sensitivity analysis of k_r to a single cell scale property (cortex cell L_p) was
677 conducted for a wide number of hydraulic anatomies (10^3 combinations of k_{AQP}, k_w and K_{PD}
678 parameter sets).

679

680 ## Accession Numbers

681 All information about the model, including the source code, is available here:
682 https://mecharoot.github.io/

683 We also developed a web application to visualize typical outputs of our model. It was
684 developed using the R Shiny framework and uses the following packages: ggplot2, ddply,
685 reshape2. The web application is accessible here:
686 https://plantmodelling.shinyapps.io/mecha/

687 MECHA was released under the GPL.2 open source licence.

Supplemental Data

Supplemental Figure S1. Figure S1. Scheme of the cell-level hydraulic network.

Supplemental Figure S2. Figure S2. Cell-scale visualization of water fluxes at different stages apoplastic barrier development for impermeable apoplastic barriers

Supplemental Figure S3. Mapping of root mean square differences of root hydraulic conductivity profiles between a reference (Doussan et al., 1998b) and simulations for sets of cell hydraulic properties widely covering the parametric space.

Supplemental Figure S4. Mapping of simulated sensitivities of root radial conductivity to cortex cell L_p, for sets of cell hydraulic properties covering the full parametric space.

Supplemental Figure S5. Impact of spatial variations of the osmotic potential in the symplast on the estimations of root hydraulic conductivity in simulated pressure clamp experiments, for perfect solute mixing in the apoplast.

Supplemental Note S1. Detailed solution of the water flow equations at the cell level.

Supplemental Note S2. On the treatment of solutes in MECHA.

Supplemental Note S3. Visualization of cell-scale composite water flow patterns at different maturity levels.

Supplemental Note S4. Systematic exploration of the parametric space to search for parameter sets reproducing experimental observations.

Supplemental Note S5. Impact of non-uniform symplastic solute concentrations on radial water fluxes.

Supplemental Data Set S1.

Supplemental Data Set S2.

Acknowledgements

We would like to thank Prof. C. Hachez for providing the root-cross section anatomical image. This work was supported by the Belgian National Fund for Scientific Research (FNRS, grant FC 84104), the Interuniversity Attraction Poles Programme-Belgian Science Policy

716 (grant IAP7/29), and the “Communauté française de Belgique-Actions de Recherches
717 Concertées” (grants ARC11/16-036 and ARC16/21-075).

718 V.C. and M.F. were supported by post-doctoral grants on the PAI MARS P7/29 project. V.C.
719 was supported by post-doctoral grants on the ARC16/21-075, FC 84104, EPPN2020 731013,
720 and EMPHASIS-PREP 739514 projects.

721 **Table 1.** Plasmodesmata frequencies within and at transitions between maize root tissue
722 types from Ma and Peterson (2001). The missing frequency information was set at the
723 average value by default.

Tissue type, or transition between tissue types	**Plasmodesmata frequency (μm^{-2})**
Epidermis to exodermis	0.54
Exodermis to cortex	1.14
Cortex	0.43
Cortex to endodermis	0.44
Endodermis	0.32
Endodermis to pericycle	0.48
Pericycle	0.35
Pericycle to stele parenchyma	0.53
Stele parenchyma	0.32
Default	0.4

724

725

Table 2. Summary of cell scale properties used in the analyses. Note that L_p and D variations were considered in the sensitivity analysis through variations around the default value. Solute reflection coefficients of cell walls and plasmodesmata were assumed to be null, while those of cell membranes equal 1 by default.

Parameter	Adjective	Value	Units	Sources or comment
Cell membrane L_p	"Default"	$5.3\ 10^{-7}$	$m\ s^{-1}MPa^{-1}$	Estimated from Ehlert *et al.* (2009) and Bret-Harte and Silk (1994)
Cell primary wall k_w	"High"	$7.7\ 10^{-8}$	$m^2s^{-1}MPa^{-1}$	Steudle and Boyer (1985)
	"Low"	$1.4\ 10^{-10}$	$m^2s^{-1}MPa^{-1}$	Tyree (1968)
Lignified / suberized cell wall $k_{w,barrier}$	"High"	$1.0\ 10^{-11}$	$m^2s^{-1}MPa^{-1}$	Poiseuille law
	"Low"	Zero	$m^2s^{-1}MPa^{-1}$	Ensures water-impermeability
Plasmodesmata K_{PD}	"High"	$3.5\ 10^{-18}$	$m^3s^{-1}MPa^{-1}$	Ginsburg and Ginzburg (1970)
	"Low"	$6.1\ 10^{-19}$	$m^3s^{-1}MPa^{-1}$	Geometrical average of range from Bret-Harte and Silk (1994)
Apoplastic solute D	"Infinite"	Infinity	$m^2\ s^{-1}$	Ensures solute perfect mixing
	"Default"	$4.0\ 10^{-11}$	$m^2\ s^{-1}$	Knipfer *et al.* (2007)

732 **Table 3.** Summary of boundary conditions used for the calculation of the root reflection
733 coefficients and for the virtual osmotic and pressure clamp experiments.

	$\psi_{p,s}$ (MPa)	$\psi_{o,s}$ (MPa)	$\psi_{p,x}$ (MPa)	$\psi_{o,x}$ (MPa)	$\psi_{o,c}$ (MPa)
Default boundary condition (no flow)	0.0	-0.02	Equilibrium pressure ($P_{r\,0}$)	-0.15	-0.7
Various $\psi_{o,s}$	0.0	-0.045 to -0.170 by -0.025 increments	$P_{r\,0}$	-0.15	-0.7
Various $\psi_{p,x}$	0.0	-0.02	$P_{r\,0}$ + 0.025 to $P_{r\,0}$ + 0.125 by 0.025 increments	-0.15	-0.7

734

735

Figure legends

Figure 1. Overview scheme of the root cross-section hydraulic anatomy approach. A transverse root microscope image (a) is treated through CellSet (c) to create the anatomical layout for cell-scale hydraulic principles (d). When coupled to cell-scale hydraulic properties (b), they form the root hydraulic anatomy (e). The computed water flow rates across individual cells (f) also yield the root radial conductivity and reflection coefficient (g).

Figure 2. Comparison of root radial hydraulic properties measured and simulated for various cell scale hydraulic properties along a root. The three simulated distances from the tip correspond to different levels of apoplastic barrier development: endodermal Casparian strip (5 cm), suberized endodermis with passage cells (25 cm), suberized endodermis and exodermal Casparian strip (50 cm). (a) Comparison between experimental k_r ranges in maize primary roots (coloured rectangles and dashed line) and k_r simulated from the cell scale in the maize hydraulic anatomy (consistent symbols across legends with impermeable and leaky apoplastic barriers in black and grey, respectively). (b) Comparison between experimental mannitol σ_r ranges in maize principal roots (coloured rectangles) and root segment σ_r arising from the cell scale in the maize hydraulic anatomy (σ_r lower than 1 were obtained with the water-permeable apoplastic barrier).

Figure 3. Impact of solute radial convection-diffusion in the apoplast on the estimations of maize root radial conductivity in simulated osmotic and pressure clamp experiments for high k_w and low K_{PD}. (a) Steady-state apoplastic osmotic potentials simulated when increasing the xylem pressure by incremental pressure clamps of 0.025 MPa for a solute diffusivity of $4\ 10^{-11}$ m^2s^{-1} (coloured curves) and an infinite diffusivity (black curves). (b) Steady-state radial water fluxes simulated in response to the incremental pressure clamps of 0.025 MPa, for 4 levels of solute diffusivity. (c) Steady-state apoplastic osmotic potentials simulated after adding mannitol in the root bathing solution by increments of 10 mOsmol for a solute diffusivity of $4\ 10^{-11}$ m^2s^{-1} (coloured curves) and an infinite diffusivity (black curves). (d) Steady-state radial water fluxes simulated in response to the increments of 10 mOsmol in the bathing solution, for 4 levels of solute diffusivity.

Figure 4. Relative radial hydraulic conductivity as a function of specific relative cell hydraulic conductivities. Relationships are shown for the fully suberized endodermis with an extra exodermal Casparian band (panels a,b,c), the suberized endodermis with 3 passage cells (panels d,e,f), and the simple endodermal Casparian band stage (panels g,h,i). In panels a, d, and g, cell properties (L_p in blue or K_{PD} in cyan) were simultaneously altered in all tissue types, while in other panels, L_p was modified in specific tissue types (in epi- and exo-dermis in dashed light blue, cortex in solid blue, endodermis in dashed dark blue, and stele cells in solid black). Panels b,e,h and c,f,i have high and low cell wall hydraulic conductivities, respectively, and low K_{PD} (see Table 2).

Figure 5. Scheme comparing major approaches to simulate water flow across root tissues. The non-exhaustive criteria listed are the separation of apoplastic and symplastic pathways, the number of dimensions attributed to the representation of longitudinally and transversally varying root properties, the compatibility with experimental anatomical layouts, and the tight coupling between solute radial distribution and water flow.

Figure 6. From anatomical segmentation to water flow simulation with CellSet and MECHA. (a) Maize root cross-section with exodermis after segmentation in CellSet. Successive cellular tissue types from the periphery: epidermis, exodermis, cortex, endodermis, pericycle, other stele cells. Water potential boundary conditions were set at the epidermis surface and in xylem vessels (dark green). Scale bar: 100 µm. (b) Simulated water fluxes in cell walls, in m s^{-1}, combining impermeable apoplastic barriers with high k_w, low K_{PD} hydraulic properties, and 0.5 MPa water potential difference between root surface and xylem, generating an average uptake flux at the root surface of 2.0 10^{-8} m s^{-1}. Note that cell wall thickness is exaggerated to improve the visualization.

References

Aroca R, Porcel R, Ruiz-Lozano J-M. 2011. Regulation of root water uptake under abiotic stress conditions. *J. Exp. Bot.* 63: 42-57.

Baluška F, Šamaj J, Napier R, Volkmann D. 1999. Maize calreticulin localizes preferentially to plasmodesmata in root apex. *Plant J.* 19: 481-488.

Band LR, Wells DM, Fozard JA, Ghetiu T, French AP, Pound MP, Wilson MH, Yu L, Li W, Hijazi HI, et al. 2014. Systems analysis of auxin transport in the *Arabidopsis* root apex. *Plant Cell* 26(3): 862-875.

Bao Y, Aggarwal P, Robbins NE, Sturrock CJ, Thompson MC, Tan HQ, Tham C, Duan L, Rodriguez PL, Vernoux T, et al. 2014. Plant roots use a patterning mechanism to position lateral root branches toward available water. *Proc. Natl. Acad. Sci. USA* 111(25): 9319-9324.

Barberon M, Vermeer JEM, De Bellis D, Wang P, Naseer S, Andersen TG, Humbel BM, Nawrath C, Takano J, Salt DE, et al. 2016. Adaptation of root function by nutrient-induced plasticity of endodermal differentiation. *Cell* 164(3): 447-459.

Barrowclough DE, Peterson CA, Steudle E. 2000. Radial hydraulic conductivity along developing onion roots. *J. Exp. Bot.* 51(344): 547-557.

Beauzamy L, Nakayama N, Boudaoud A. 2014. Flowers under pressure: ins and outs of turgor regulation in development. *Ann. Bot.* 114(7): 1517-1533.

Bell K, Oparka K. 2011. Imaging plasmodesmata. *Protoplasma* 248: 9-25.

Boursiac Y, Boudet J, Postaire O, Luu D-T, Tournaire-Roux C, Maurel C. 2008. Stimulus-induced downregulation of root water transport involves reactive oxygen species-activated cell signalling and plasma membrane intrinsic protein internalization. *Plant J.* 56(2): 207-218.

Bramley H, Turner NC, Turner DW, Tyerman SD. 2007. Comparison between gradient-dependent hydraulic conductivities of roots using the root pressure probe: the role of pressure propagations and implications for the relative roles of parallel radial pathways. *Plant Cell Environ.* 30(7): 861-874.

Bret-Harte MS, Silk WK. 1994. Nonvascular, symplasmic diffusion of sucrose cannot satisfy the carbon demands of growth in the primary root tip of *Zea mays* L. *Plant Physiol.* 105: 19-33.

Brunkard JO, Zambryski PC. 2017. Plasmodesmata enable multicellularity: new insights into their evolution, biogenesis, and functions in development and immunity. *Curr. Opin. Plant Biol.* 35: 76-83.

Brynjarsdóttir J, O'Hagan A. 2014. Learning about physical parameters: the importance of model discrepancy. *Inverse Problems* 30(11): 114007.

Caldeira CF, Jeanguenin L, Chaumont F, Tardieu F. 2014. Circadian rhythms of hydraulic conductance and growth are enhanced by drought and improve plant performance. *Nat. Commun.* 5.

Cattivelli L, Rizza F, Badeck F-W, Mazzucotelli E, Mastrangelo AM, Francia E, Marè C, Tondelli A, Stanca AM. 2008. Drought tolerance improvement in crop plants: An integrated view from breeding to genomics. *Field Crops Research* 105(1): 1-14.

Chaumont F, Tyerman SD. 2014. Aquaporins: highly regulated channels controlling plant water relations. *Plant Physiol.* 164(4): 1600-1618.

Clarkson DT, Robards AW, Sanderson J. 1971. The tertiary endodermis in barley roots: Fine structure in relation to radial transport of ions and water. *Planta* 96(4): 292-305.

Clarkson DT, Robards AW, Stephens JE, Stark M. 1987. Suberin lamellae in the hypodermis of maize (*Zea mays*) roots; development and factors affecting the permeability of hypodermal layers. *Plant Cell Environ.* 10(1): 83-93.

Couvreur V, Kandelous MM, Sanden BL, Lampinen BD, Hopmans JW. 2016. Downscaling transpiration rate from field to tree scale. *Agr. Forest Meteorol.* 221: 71-77.

Couvreur V, Vanderborght J, Beff L, Javaux M. 2014. Horizontal soil water potential heterogeneity: Simplifying approaches for crop water dynamics models. *Hydrol. Earth Syst. Sc.* 18(5): 1723-1743.

837 Deng J, Xiong T, Wang H, Zheng A, Wang Y. 2016. Effects of cellulose, hemicellulose, and lignin on the
838 structure and morphology of porous carbons. *ACS Sustain. Chem. Eng.* 4(7): 3750-3756.
839 Dietrich D, Pang L, Kobayashi A, Fozard JA, Boudolf V, Bhosale R, Antoni R, Nguyen T, Hiratsuka S,
840 Fujii N, et al. 2017. Root hydrotropism is controlled via a cortex-specific growth mechanism.
841 *Nature Plants* 3: 17057.
842 Doblas VG, Smakowska-Luzan E, Fujita S, Alassimone J, Barberon M, Madalinski M, Belkhadir Y,
843 Geldner N. 2017. Root diffusion barrier control by a vasculature-derived peptide binding to
844 the SGN3 receptor. *Science* 355(6322): 280-284.
845 Doussan C, Pages L, Vercambre G. 1998a. Modelling of the hydraulic architecture of root systems: An
846 integrated approach to water absorption - Model description. *Ann. Bot.-London* 81(2): 213-
847 223.
848 Doussan C, Vercambre G, Pages L. 1998b. Modelling of the hydraulic architecture of root systems: An
849 integrated approach to water absorption - Distribution of axial and radial conductances in
850 maize. *Ann. Bot.-London* 81(2): 225-232.
851 Draye X, Kim Y, Lobet G, Javaux M. 2010. Model-assisted integration of physiological and
852 environmental constraints affecting the dynamic and spatial patterns of root water uptake
853 from soils. *J. Exp. Bot.* 61(8): 2145-2155.
854 Ehlert C, Maurel C, Tardieu F, Simonneau T. 2009. Aquaporin-mediated reduction in maize root
855 hydraulic conductivity impacts cell turgor and leaf elongation even without changing
856 transpiration. *Plant Physiol.* 150: 1093-1104.
857 Enns LC, Canny MJ, McCully ME. 2000. An investigation of the role of solutes in the xylem sap and in
858 the xylem parenchyma as the source of root pressure. *Protoplasma* 211: 183-197.
859 Enstone DE, Peterson CA. 2005. Suberin lamella development in maize seedling roots grown in
860 aerated and stagnant conditions. *Plant Cell Environ.* 28(4): 444-455.
861 Enstone DE, Peterson CA, Ma F. 2002. Root endodermis and exodermis: Structure, function, and
862 responses to the environment. *J. Plant Growth Regul.* 21(4): 335-351.
863 Feddes RA, Kowalik PJ, Zaradny H. 1978. *Simulation of field water use and crop yield*.
864 Fiscus EL, Kramer PJ. 1975. General model for osmotic and pressure-induced flow in plant roots. *Proc.
865 Natn. Acad. Sci. U.S.A.* 72(8): 3114-3118.
866 Foster KJ, Miklavcic SJ. 2016. Modeling Root Zone Effects on Preferred Pathways for the Passive
867 Transport of Ions and Water in Plant Roots. *Front. Plant Sci.* 7:914.
868 Foster KJ, Miklavcic SJ. 2017. A Comprehensive Biophysical Model of Ion and Water Transport in
869 Plant Roots. I. Clarifying the Roles of Endodermal Barriers in the Salt Stress Response. *Front.
870 Plant Sci.* 8:1326.
871 Frensch J, Steudle E. 1989. Axial and radial hydraulic resistance to roots of maize (*Zea mays L*). *Plant
872 Physiol.* 91(2): 719-726.
873 Fritz M, Ehwald R. 2011. Mannitol permeation and radial flow of water in maize roots. *New Phytol.*
874 189(1): 210-217.
875 Ginsburg H, Ginzburg BZ. 1970. Radial water and solute flows in roots of *Zea mays*: I. Water Flow. *J.
876 Exp. Bot.* 21(3): 580-592.
877 Hachez C, Moshelion M, Zelazny E, Cavez D, Chaumont F. 2006. Localization and quantification of
878 plasma membrane aquaporin expression in maize primary root: A clue to understanding their
879 role as cellular plumbers. *Plant Mol. Biol.* 62(1-2): 305-323.
880 Hachez C, Veselov D, Ye Q, Reinhardt H, Knipfer T, Fricke W, Chaumont F. 2012. Short-term control of
881 maize cell and root water permeability through plasma membrane aquaporin isoforms. *Plant
882 Cell Environ.* 35(1): 185-198.
883 Hamza M, Aylmore L. 1992. Soil solute concentration and water uptake by single lupin and radish
884 plant roots. *Plant Soil* 145: 187–196.
885 Javaux M, Couvreur V, Vanderborght J, Vereecken H. 2013. Root water uptake: From 3D biophysical
886 processes to macroscopic modeling approaches. *Vadose Zone J.* 12(VZJ Anniversary Issue): 16
887 pp.

888 Javaux M, Schroder T, Vanderborght J, Vereecken H. 2008. Use of a three-dimensional detailed
889 modeling approach for predicting root water uptake. *Vadose Zone J.* 7(3): 1079-1088.
890 Katchalsky A, Curran PF. 1967. *Nonequilibrium thermodynamics in biophysics*. Cambridge: Harvard
891 University Press.
892 Knipfer T, Fricke W. 2010. Root pressure and a solute reflection coefficient close to unity exclude a
893 purely apoplastic pathway of radial water transport in barley (*Hordeum vulgare*). *New Phytol.*
894 187(1): 159-170.
895 Knipfer T, Das D, Steudle E. 2007. During measurements of root hydraulics with pressure probes, the
896 contribution of unstirred layers is minimized in the pressure relaxation mode: comparison
897 with pressure clamp and high-pressure flowmeter. *Plant Cell Environ.* 30: 845-860.
898 Lee J-Y, Wang X, Cui W, et al. A Plasmodesmata-Localized Protein Mediates Crosstalk between Cell-
899 to-Cell Communication and Innate Immunity in Arabidopsis. The Plant Cell. 2011;23(9):3353-
900 3373.
901 Ma F, Peterson CA. 2001. Frequencies of plasmodesmata in *Allium cepa L*. roots: implications for
902 solute transport pathways. *J. Exp. Bot.* 52: 1051-1061.
903 Maule AJ. 2008. Plasmodesmata: structure, function and biogenesis. *Curr. Opin. Plant Biol.* 11(6):
904 680-686.
905 Maurel C, Chrispeels MJ. 2001. Aquaporins. A molecular entry into plant water relations. *Plant*
906 *Physiol.* 125(1): 135-138.
907 McElrone AJ, Bichler J, Pockman WT, Addington RN, Linder CR, Jackson RB. 2007. Aquaporin-
908 mediated changes in hydraulic conductivity of deep tree roots accessed via caves. *Plant Cell*
909 *Environ.* 30(11): 1411-1421.
910 Meunier F, Couvreur V, Draye X, Vanderborght J, Javaux M. 2017a. Towards quantitative root
911 hydraulic phenotyping: novel mathematical functions to calculate plant-scale hydraulic
912 parameters from root system functional and structural traits. *J. of Mathematical Biol*: 38 pp.
913 Meunier F, Rothfuss Y, Bariac T, Biron P, Richard P, Durand J-L, Couvreur V, Vanderborght J, Javaux
914 M. 2017b. Measuring and modeling hydraulic lift of *Lolium multiflorum* using stable water
915 isotopes. *Vadose Zone J.*: 15 pp.
916 Meunier F, Draye X, Vanderborght J, Javaux M, Couvreur V. 2017c. A hybrid analytical-numerical
917 method for solving water flow equations in root hydraulic architectures. *Appl. Math. Model.*
918 52: 648-663.
919 Parent B, Hachez C, Redondo E, Simonneau T, Chaumont F, Tardieu F. 2009. Drought and abscisic acid
920 effects on aquaporin content translate into changes in hydraulic conductivity and leaf growth
921 rate: A trans-scale approach. *Plant Physiol.* 149(4): 2000-2012.
922 Pokhrel P, Gupta HV. 2010. On the use of spatial regularization strategies to improve calibration of
923 distributed watershed models. *Water Resour. Res.* 46: 17 pp.
924 Postma JA, Kuppe C, Owen MR, Mellor N, Griffiths M, Bennett MJ, Lynch JP, Watt M. 2017.
925 OpenSimRoot: widening the scope and application of root architectural models. *New Phytol.*
926 215(3): 1274-1286.
927 Pound MP, French AP, Wells DM, Bennett MJ, Pridmore TP. 2012. CellSeT: novel software to extract
928 and analyze structured networks of plant cells from confocal images. *The Plant Cell* 24(4):
929 1353-1361.
930 Pusch W, Woermann D. 1970. Study of the Interrelation Between Reflection Coefficient and Solute
931 Rejection Efficiency Using a Strong Basic Anion Exchange Membrane. *Ber. Bunsenges. phys.*
932 *Chem.*, 74: 444-449
933 Roberts AG, Oparka KJ. 2003. Plasmodesmata and the control of symplastic transport. *Plant Cell*
934 *Environ.* 26(1): 103-124.
935 Ross-Elliott TJ, Jensen KH, Haaning KS, Wager BM, Knoblauch J, Howell AH, Mullendore DL, Monteith
936 AG, Paultre D, Yan D, Otero S, Bourdon M, Sager R, Lee J-Y, Helariutta Y, Knoblauch M,
937 Oparka KJ. 2017. Phloem unloading in *Arabidopsis* roots is convective and regulated by the
938 phloem-pole pericycle. eLife 6:e24125.

939 Rygol J, Pritchard J, Zhu JJ, Tomos AD, Zimmermann U. 1993. Transpiration induces radial turgor
940 pressure gradients in wheat and maize roots. *Plant Physiol.* 103: 493-500.
941 Sanderson J. 1983. Water-uptake by different regions of the barley root - pathways of radial flow in
942 relation to development of the endodermis. *J. Exp. Bot.* 34(140): 240-253.
943 Schoppach R, Wauthelet D, Jeanguenin L, Sadok W. 2014. Conservative water use under high
944 evaporative demand associated with smaller root metaxylem and limited trans-membrane
945 water transport in wheat. *Funct. Plant Bio.* 41(3): 257-269.
946 Schröder N, Lazarovitch N, Vanderborght J, Vereecken H, Javaux M. 2014. Linking transpiration
947 reduction to rhizosphere salinity using a 3D coupled soil-plant model. *Plant Soil* 377(1-2):
948 277-293.
949 Sevilem I, Miyashima S, Helariutta Y. 2013. Cell-to-cell communication via plasmodesmata in vascular
950 plants. *Cell Adhesion & Migration* 7(1): 27-32.
951 Sperry JS, Hacke UG, Oren R, Comstock JP. 2002. Water deficits and hydraulic limits to leaf water
952 supply. *Plant, Cell and Environment* 25(2): 251-263.
953 Steudle E, Boyer JS. 1985. Hydraulic resistance to radial water flow in growing hypocotyl of soybean
954 measured by a new pressure-perfusion technique. *Planta* 164(2): 189-200.
955 Steudle E, Frensch J. 1989. Osmotic responses of maize roots. *Planta* 177(3): 281-295.
956 Steudle E, Jeschke WD. 1983. Water transport in barley roots : Measurements of root pressure and
957 hydraulic conductivity of roots in parallel with turgor and hydraulic conductivity of root cells.
958 *Planta* 158: 237-248.
959 Steudle E, Oren R, Schulze ED. 1987. Water transport in maize roots - Measurement of hydraulic
960 conductivity, solute permeability, and of reflection coefficients of excised roots using the
961 root pressure probe. *Plant Physiol.* 84(4): 1220-1232.
962 Steudle E, Peterson CA. 1998. How does water get through roots? *J. Exp. Bot.* 49(322): 775-788.
963 Terry BR, Robards AW. 1987. Hydrodynamic radius alone govems the mobility of molecules through
964 plasmodesmata. *Planta* 171: 145-157.
965 Tornroth-Horsefield S, Wang Y, Hedfalk K, Johanson U, Karlsson M, Tajkhorshid E, Neutze R, Kjellbom
966 P. 2006. Structural mechanism of plant aquaporin gating. *Nature* 439(7077): 688-694.
967 Tournaire-Roux C, Sutka M, Javot H, Gout E, Gerbeau P, Luu DT, Bligny R, Maurel C. 2003. Cytosolic
968 pH regulates root water transport during anoxic stress through gating of aquaporins. *Nature*
969 425(6956): 393-397.
970 Tyree MT. 1968. Determination of transport constants of isolated *Nitella* cell walls. *Canad. J. Bot.* 46:
971 317-327.
972 Varney GT, Canny MJ. 1993. Rates of water-uptake into the mature root-system of maize plants. *New*
973 *Phytol.* 123(4): 775-786.
974 Von Wangenheim D, Goh T, Dietrich D, Bennett MJ. 2017. Plant biology: building barriers... in Roots.
975 *Current Biology* 27(5): R172-R174.
976 Warmbrodt RD. 1985. Studies on the root of *Zea mays L*.-structure of the adventitious roots with
977 respect to phloem unloading. *Bot. Gaz.* 146(2): 169-180.
978 Ye Q, Steudle E. 2006. Oxidative gating of water channels (aquaporins) in corn roots. *Plant Cell*
979 *Environ.* 29(4): 459-470.
980 Zarebanadkouki M, Kroener E, Kaestner A, Carminati A. 2014. Visualization of root water uptake:
981 Quantification of deuterated water transport in roots using neutron radiography and
982 numerical modeling. *Plant Physiol.*
983 Zarebanadkouki M, Meunier F, Couvreur V, Cesar J, Javaux M, Carminati A. 2016. Estimation of the
984 hydraulic conductivities of lupine roots by inverse modelling of high-resolution
985 measurements of root water uptake. *Ann. Bot.*
986 Zhu GL, Steudle E. 1991. Water transport across maize roots: simultaneous measurement of flows at
987 the cell and root level by double pressure probe technique. *Plant Physiol.* 95(1): 305-315.
988 Zimmermann HM, Hartmann K, Schreiber L, Steudle E. 2000. Chemical composition of apoplastic
989 transport barriers in relation to radial hydraulic conductivity of corn roots (Zea mays L.).
990 Planta 210: 302-311.

991 Zwieniecki MA, Thompson MV, Holbrook MN. 2002. Understanding the hydraulics of porous pipes:
992 Tradeoffs between water uptake and root length utilization. J. Plant Growth Regul. 21: 315-
993 323.
994

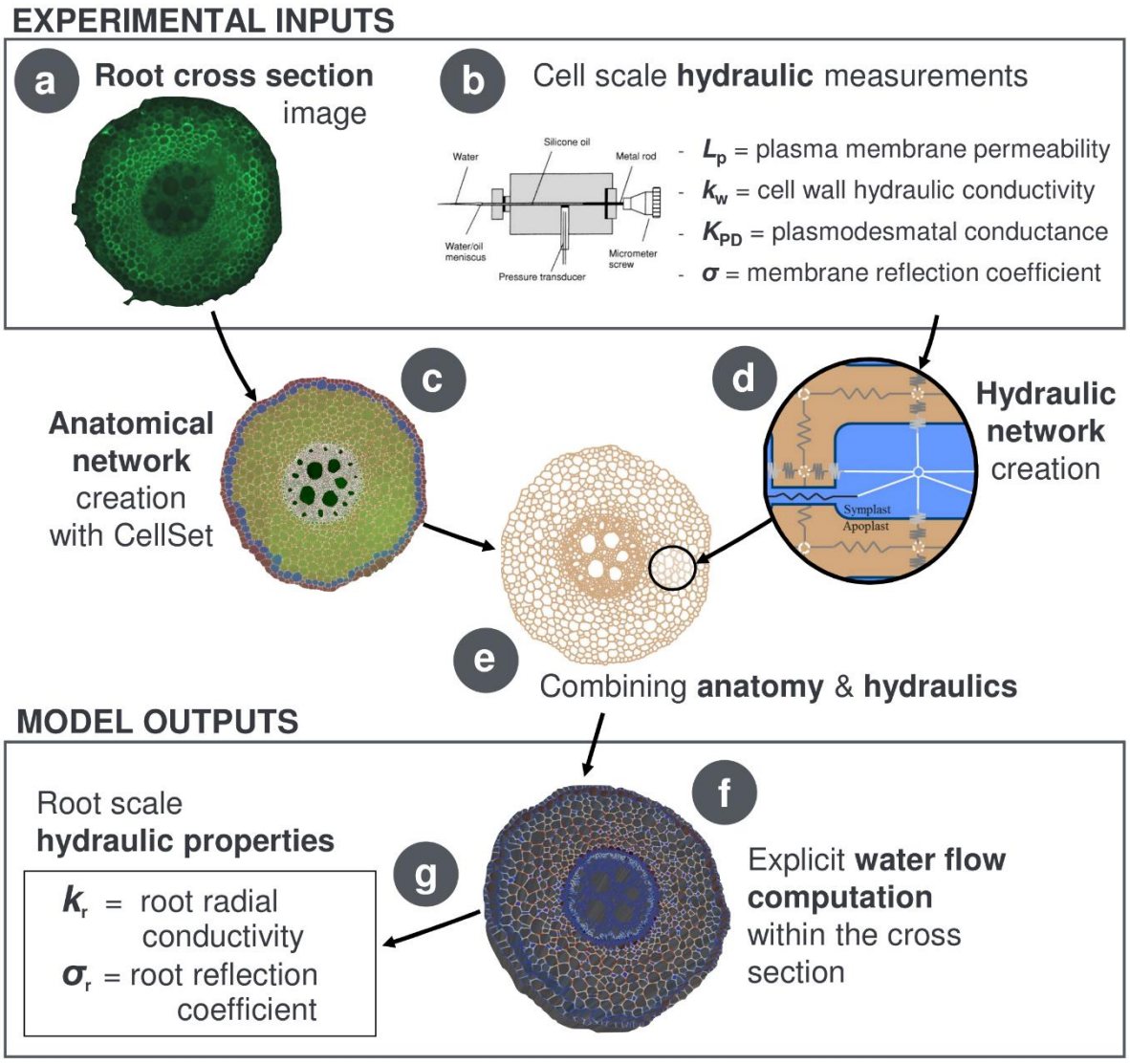

Figure 1. Overview scheme of the root cross-section hydraulic anatomy approach. A transverse root microscope image (a) is treated through CellSet (c), in order to create the anatomical layout for cell-scale hydraulic principles (d). When coupled to cell-scale hydraulic properties (b), they form the root hydraulic anatomy (e). The computed water flow rates across individual cells (f) also yield the root radial conductivity and reflection coefficient (g).

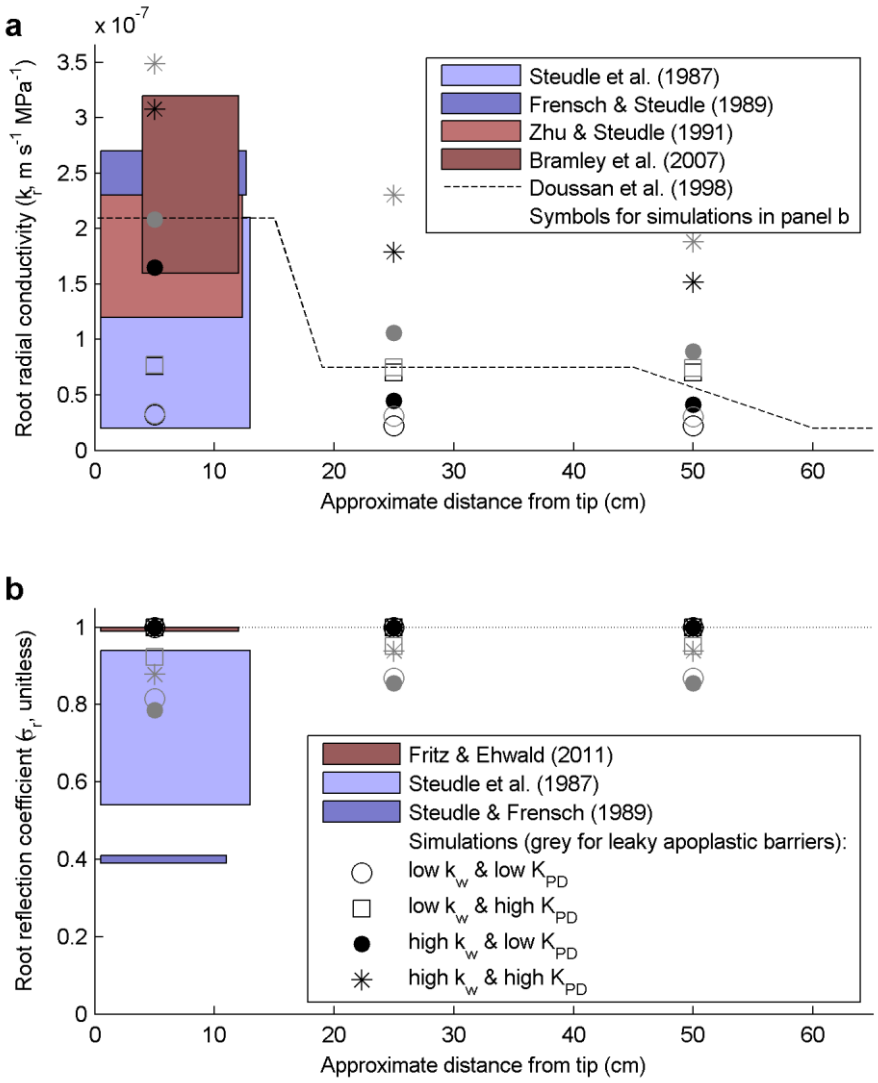

Figure 2. Comparison of root radial hydraulic properties measured and simulated for various cell scale hydraulic properties along a root. The three simulated distances from the tip correspond to different levels of apoplastic barrier development: endodermal Casparian strip (5 cm), suberized endodermis with passage cells (25 cm), suberized endodermis and exodermal Casparian strip (50 cm). (a) Comparison between experimental k_r ranges in maize primary roots (coloured rectangles and dashed line) and k_r simulated from the cell scale in the maize hydraulic anatomy (consistent symbols across legends with impermeable and leaky apoplastic barriers in black and grey, respectively). (b) Comparison between experimental mannitol σ_r ranges in maize principal roots (coloured rectangles) and root segment σ_r arising from the cell scale in the maize hydraulic anatomy (σ_r lower than 1 were obtained with the water-permeable apoplastic barrier).

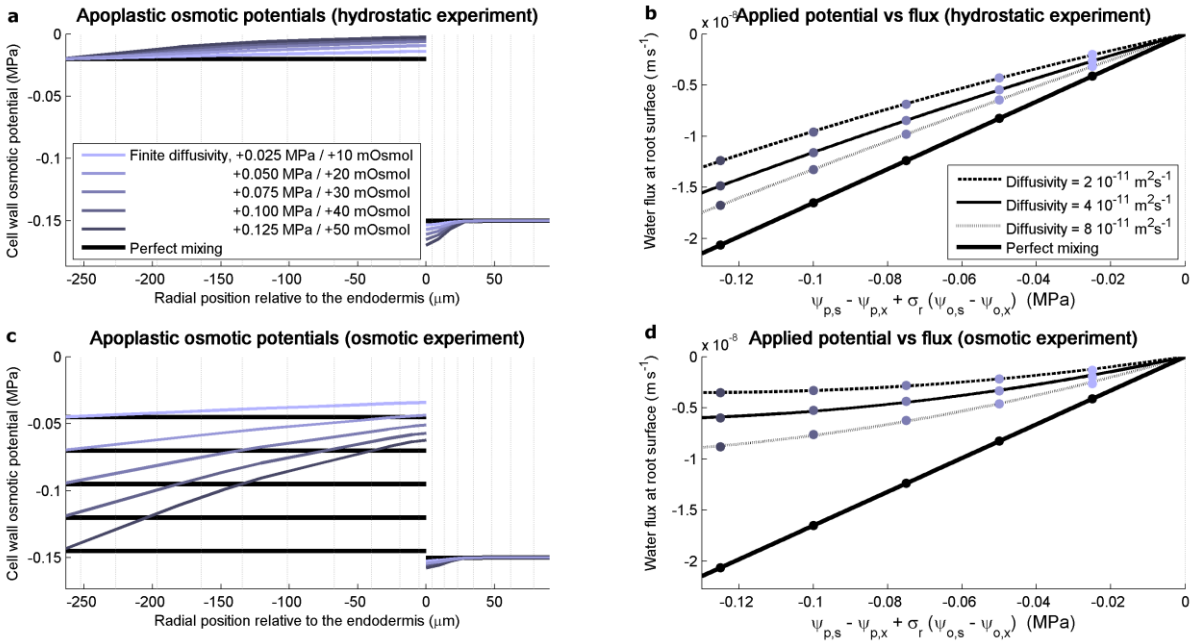

Figure 3. Impact of solute radial convection-diffusion in the apoplast on the estimations of maize root radial conductivity in simulated osmotic and pressure clamp experiments, for high k_w and low K_{PD}. (a) Steady-state apoplastic osmotic potentials simulated when increasing the xylem pressure by incremental pressure clamps of 0.025 MPa for a solute diffusivity of 4 10^{-11} m^2s^{-1} (coloured curves) and an infinite diffusivity (black curves). (b) Steady-state radial water fluxes simulated in response to the incremental pressure clamps of 0.025 MPa, for 4 levels of solute diffusivity. (c) Steady-state apoplastic osmotic potentials simulated after adding mannitol in the root bathing solution by increments of 10 mOsmol for a solute diffusivity of 4 10^{-11} m^2s^{-1} (coloured curves) and an infinite diffusivity (black curves). (d) Steady-state radial water fluxes simulated in response to the increments of 10 mOsmol in the bathing solution, for 4 levels of solute diffusivity.

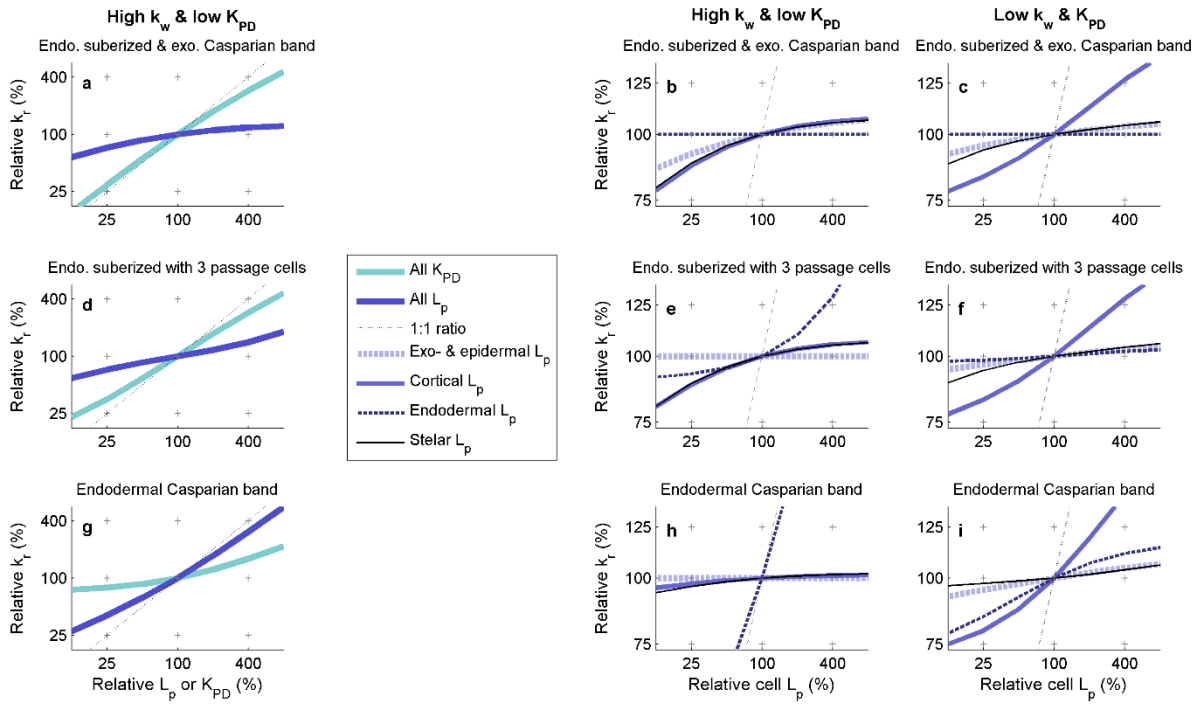

Figure 4. Relative radial hydraulic conductivity as a function of specific relative cell hydraulic conductivities, for the fully suberized endodermis with an extra exodermal Casparian band (panels a,b,c), the suberized endodermis with 3 passage cells (panels d,e,f), and the simple endodermal Casparian band stage (panels g,h,i). In panels a, d, and g, cell properties (L_p in blue or K_{PD} in cyan) were simultaneously altered in all tissue types, while in other panels, L_p was modified in specific tissue types (in epi- and exo-dermis in dashed light blue, cortex in solid blue, endodermis in dashed dark blue, and stele cells in solid black). Panels b,e,h and c,f,i have high and low cell wall hydraulic conductivities, respectively, and low K_{PD} (see Tab. 2).

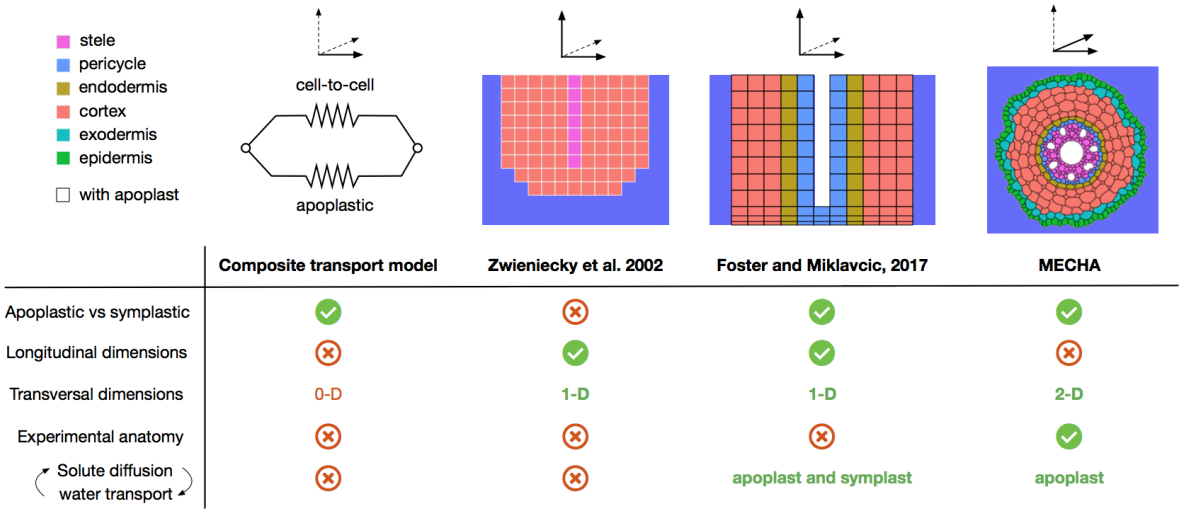

Figure 5. Scheme comparing major approaches to simulate water flow across root tissues. The non-exhaustive criteria listed are the separation apoplastic and symplastic pathways, the number of dimensions attributed to the representation of longitudinally and transversally varying root properties, the compatibility with experimental anatomical layouts, and the tight coupling between solute radial distribution and water flow.

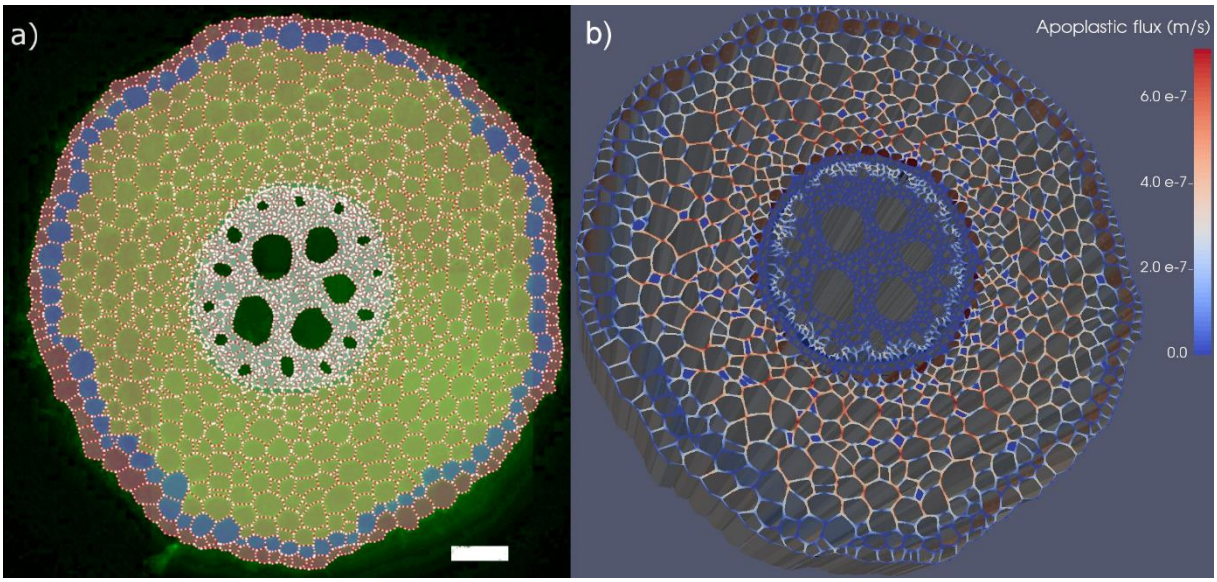

Figure 6. From anatomical segmentation to water flow simulation with CellSet and MECHA. (a) Maize root cross-section with exodermis after segmentation in CellSet. Successive cellular tissue types from the periphery: epidermis, exodermis, cortex, endodermis, pericycle, other stele cells. Water potential boundary conditions were set at the epidermis surface and in xylem vessels (dark green). Scale bar: 100 µm. (b) Simulated water fluxes in cell walls, in m s^{-1}, combining impermeable apoplastic barriers with high k_w, low K_{PD} hydraulic properties, and 0.5 MPa water potential difference between root surface and xylem, generating an average uptake flux at the root surface of 2.0 10^{-8} m s^{-1}. Note that cell wall thickness is exaggerated to improve the visualization.

Parsed Citations

Aroca R, Porcel R, Ruiz-Lozano J-M. 2011. Regulation of root water uptake under abiotic stress conditions. J. Exp. Bot. 63: 42-57.
Pubmed: Author and Title
Google Scholar: Author Only Title Only Author and Title

Baluška F, Šamaj J, Napier R, Volkmann D. 1999. Maize calreticulin localizes preferentially to plasmodesmata in root apex. Plant J. 19: 481-488.
Pubmed: Author and Title
Google Scholar: Author Only Title Only Author and Title

Band LR, Wells DM, Fozard JA, Ghetiu T, French AP, Pound MP, Wilson MH, Yu L, Li W, Hijazi HI, et al. 2014. Systems analysis of auxin transport in the Arabidopsis root apex. Plant Cell 26(3): 862-875.
Pubmed: Author and Title
Google Scholar: Author Only Title Only Author and Title

Bao Y, Aggarwal P, Robbins NE, Sturrock CJ, Thompson MC, Tan HQ, Tham C, Duan L, Rodriguez PL, Vernoux T, et al. 2014. Plant roots use a patterning mechanism to position lateral root branches toward available water. Proc. Natl. Acad. Sci. USA 111(25): 9319-9324.
Pubmed: Author and Title
Google Scholar: Author Only Title Only Author and Title

Barberon M, Vermeer JEM, De Bellis D, Wang P, Naseer S, Andersen TG, Humbel BM, Nawrath C, Takano J, Salt DE, et al. 2016. Adaptation of root function by nutrient-induced plasticity of endodermal differentiation. Cell 164(3): 447-459.
Pubmed: Author and Title
Google Scholar: Author Only Title Only Author and Title

Barrowclough DE, Peterson CA, Steudle E. 2000. Radial hydraulic conductivity along developing onion roots. J. Exp. Bot. 51(344): 547-557.
Pubmed: Author and Title
Google Scholar: Author Only Title Only Author and Title

Beauzamy L, Nakayama N, Boudaoud A. 2014. Flowers under pressure: ins and outs of turgor regulation in development. Ann. Bot. 114(7): 1517-1533.
Pubmed: Author and Title
Google Scholar: Author Only Title Only Author and Title

Bell K, Oparka K. 2011. Imaging plasmodesmata. Protoplasma 248: 9-25.
Pubmed: Author and Title
Google Scholar: Author Only Title Only Author and Title

Boursiac Y, Boudet J, Postaire O, Luu D-T, Tournaire-Roux C, Maurel C. 2008. Stimulus-induced downregulation of root water transport involves reactive oxygen species-activated cell signalling and plasma membrane intrinsic protein internalization. Plant J. 56(2): 207-218.
Pubmed: Author and Title
Google Scholar: Author Only Title Only Author and Title

Bramley H, Turner NC, Turner DW, Tyerman SD. 2007. Comparison between gradient-dependent hydraulic conductivities of roots using the root pressure probe: the role of pressure propagations and implications for the relative roles of parallel radial pathways. Plant Cell Environ. 30(7): 861-874.
Pubmed: Author and Title
Google Scholar: Author Only Title Only Author and Title

Bret-Harte MS, Silk WK. 1994. Nonvascular, symplasmic diffusion of sucrose cannot satisfy the carbon demands of growth in the primary root tip of Zea mays L. Plant Physiol. 105: 19-33.
Pubmed: Author and Title
Google Scholar: Author Only Title Only Author and Title

Brunkard JO, Zambryski PC. 2017. Plasmodesmata enable multicellularity: new insights into their evolution, biogenesis, and functions in development and immunity. Curr. Opin. Plant Biol. 35: 76-83.
Pubmed: Author and Title
Google Scholar: Author Only Title Only Author and Title

Brynjarsdóttir J, O'Hagan A. 2014. Learning about physical parameters: the importance of model discrepancy. Inverse Problems 30(11): 114007.
Pubmed: Author and Title
Google Scholar: Author Only Title Only Author and Title

Caldeira CF, Jeanguenin L, Chaumont F, Tardieu F. 2014. Circadian rhythms of hydraulic conductance and growth are enhanced by drought and improve plant performance. Nat. Commun. 5.
Pubmed: Author and Title
Google Scholar: Author Only Title Only Author and Title

Cattivelli L, Rizza F, Badeck F-W, Mazzucotelli E, Mastrangelo AM, Francia E, Marè C, Tondelli A, Stanca AM. 2008. Drought tolerance

improvement in crop plants: An integrated view from breeding to genomics. Field Crops Research 105(1): 1-14.
Pubmed: Author and Title
Google Scholar: Author Only Title Only Author and Title

Chaumont F, Tyerman SD. 2014. Aquaporins: highly regulated channels controlling plant water relations. Plant Physiol. 164(4): 1600-1618.
Pubmed: Author and Title
Google Scholar: Author Only Title Only Author and Title

Clarkson DT, Robards AW, Sanderson J. 1971. The tertiary endodermis in barley roots: Fine structure in relation to radial transport of ions and water. Planta 96(4): 292-305.
Pubmed: Author and Title
Google Scholar: Author Only Title Only Author and Title

Clarkson DT, Robards AW, Stephens JE, Stark M. 1987. Suberin lamellae in the hypodermis of maize (Zea mays) roots; development and factors affecting the permeability of hypodermal layers. Plant Cell Environ. 10(1): 83-93.
Pubmed: Author and Title
Google Scholar: Author Only Title Only Author and Title

Couvreur V, Kandelous MM, Sanden BL, Lampinen BD, Hopmans JW. 2016. Downscaling transpiration rate from field to tree scale. Agr. Forest Meteorol. 221: 71-77.
Pubmed: Author and Title
Google Scholar: Author Only Title Only Author and Title

Couvreur V, Vanderborght J, Beff L, Javaux M. 2014. Horizontal soil water potential heterogeneity: Simplifying approaches for crop water dynamics models. Hydrol. Earth Syst. Sc. 18(5): 1723-1743.
Pubmed: Author and Title
Google Scholar: Author Only Title Only Author and Title

Deng J, Xiong T, Wang H, Zheng A, Wang Y. 2016. Effects of cellulose, hemicellulose, and lignin on the structure and morphology of porous carbons. ACS Sustain. Chem. Eng. 4(7): 3750-3756.
Pubmed: Author and Title
Google Scholar: Author Only Title Only Author and Title

Dietrich D, Pang L, Kobayashi A, Fozard JA, Boudolf V, Bhosale R, Antoni R, Nguyen T, Hiratsuka S, Fujii N, et al. 2017. Root hydrotropism is controlled via a cortex-specific growth mechanism. Nature Plants 3: 17057.
Pubmed: Author and Title
Google Scholar: Author Only Title Only Author and Title

Doblas VG, Smakowska-Luzan E, Fujita S, Alassimone J, Barberon M, Madalinski M, Belkhadir Y, Geldner N. 2017. Root diffusion barrier control by a vasculature-derived peptide binding to the SGN3 receptor. Science 355(6322): 280-284.

Doussan C, Pages L, Vercambre G. 1998a. Modelling of the hydraulic architecture of root systems: An integrated approach to water absorption - Model description. Ann. Bot.-London 81(2): 213-223.
Pubmed: Author and Title
Google Scholar: Author Only Title Only Author and Title

Doussan C, Vercambre G, Pages L. 1998b. Modelling of the hydraulic architecture of root systems: An integrated approach to water absorption - Distribution of axial and radial conductances in maize. Ann. Bot.-London 81(2): 225-232.
Pubmed: Author and Title
Google Scholar: Author Only Title Only Author and Title

Draye X, Kim Y, Lobet G, Javaux M. 2010. Model-assisted integration of physiological and environmental constraints affecting the dynamic and spatial patterns of root water uptake from soils. J. Exp. Bot. 61(8): 2145-2155.
Pubmed: Author and Title
Google Scholar: Author Only Title Only Author and Title

Ehlert C, Maurel C, Tardieu F, Simonneau T. 2009. Aquaporin-mediated reduction in maize root hydraulic conductivity impacts cell turgor and leaf elongation even without changing transpiration. Plant Physiol. 150: 1093-1104.
Pubmed: Author and Title
Google Scholar: Author Only Title Only Author and Title

Enns LC, Canny MJ, McCully ME. 2000. An investigation of the role of solutes in the xylem sap and in the xylem parenchyma as the source of root pressure. Protoplasma 211: 183-197.
Pubmed: Author and Title
Google Scholar: Author Only Title Only Author and Title

Enstone DE, Peterson CA. 2005. Suberin lamella development in maize seedling roots grown in aerated and stagnant conditions. Plant Cell Environ. 28(4): 444-455.
Pubmed: Author and Title
Google Scholar: Author Only Title Only Author and Title

Enstone DE, Peterson CA, Ma F. 2002. Root endodermis and exodermis: Structure, function, and responses to the environment. J. Plant Growth Regul. 21(4): 335-351.
Pubmed: Author and Title

Google Scholar: Author Only Title Only Author and Title

Feddes RA, Kowalik PJ, Zaradny H. 1978. Simulation of field water use and crop yield.

Fiscus EL, Kramer PJ. 1975. General model for osmotic and pressure-induced flow in plant roots. Proc. Natn. Acad. Sci. U.S.A. 72(8): 3114-3118.
Pubmed: Author and Title
Google Scholar: Author Only Title Only Author and Title

Foster KJ, Miklavcic SJ. 2016. Modeling Root Zone Effects on Preferred Pathways for the Passive Transport of Ions and Water in Plant Roots. Front. Plant Sci. 7:914.
Pubmed: Author and Title
Google Scholar: Author Only Title Only Author and Title

Foster KJ, Miklavcic SJ. 2017. A Comprehensive Biophysical Model of Ion and Water Transport in Plant Roots. I. Clarifying the Roles of Endodermal Barriers in the Salt Stress Response. Front. Plant Sci. 8:1326.
Pubmed: Author and Title
Google Scholar: Author Only Title Only Author and Title

Frensch J, Steudle E. 1989. Axial and radial hydraulic resistance to roots of maize (Zea mays L). Plant Physiol. 91(2): 719-726.
Pubmed: Author and Title
Google Scholar: Author Only Title Only Author and Title

Fritz M, Ehwald R. 2011. Mannitol permeation and radial flow of water in maize roots. New Phytol. 189(1): 210-217.
Pubmed: Author and Title
Google Scholar: Author Only Title Only Author and Title

Ginsburg H, Ginzburg BZ. 1970. Radial water and solute flows in roots of Zea mays: I. Water Flow. J. Exp. Bot. 21(3): 580-592.
Pubmed: Author and Title
Google Scholar: Author Only Title Only Author and Title

Hachez C, Moshelion M, Zelazny E, Cavez D, Chaumont F. 2006. Localization and quantification of plasma membrane aquaporin expression in maize primary root: A clue to understanding their role as cellular plumbers. Plant Mol. Biol. 62(1-2): 305-323.
Pubmed: Author and Title
Google Scholar: Author Only Title Only Author and Title

Hachez C, Veselov D, Ye Q, Reinhardt H, Knipfer T, Fricke W, Chaumont F. 2012. Short-term control of maize cell and root water permeability through plasma membrane aquaporin isoforms. Plant Cell Environ. 35(1): 185-198.
Pubmed: Author and Title
Google Scholar: Author Only Title Only Author and Title

Hamza M, Aylmore L. 1992. Soil solute concentration and water uptake by single lupin and radish plant roots. Plant Soil 145: 187–196.
Pubmed: Author and Title
Google Scholar: Author Only Title Only Author and Title

Javaux M, Couvreur V, Vanderborght J, Vereecken H. 2013. Root water uptake: From 3D biophysical processes to macroscopic modeling approaches. Vadose Zone J. 12(VZJ Anniversary Issue): 16 pp.
Pubmed: Author and Title
Google Scholar: Author Only Title Only Author and Title

Javaux M, Schroder T, Vanderborght J, Vereecken H. 2008. Use of a three-dimensional detailed modeling approach for predicting root water uptake. Vadose Zone J. 7(3): 1079-1088.
Pubmed: Author and Title
Google Scholar: Author Only Title Only Author and Title

Katchalsky A, Curran PF. 1967. Nonequilibrium thermodynamics in biophysics. Cambridge: Harvard University Press.
Pubmed: Author and Title
Google Scholar: Author Only Title Only Author and Title

Knipfer T, Fricke W. 2010. Root pressure and a solute reflection coefficient close to unity exclude a purely apoplastic pathway of radial water transport in barley (Hordeum vulgare). New Phytol. 187(1): 159-170.
Pubmed: Author and Title
Google Scholar: Author Only Title Only Author and Title

Knipfer T, Das D, Steudle E. 2007. During measurements of root hydraulics with pressure probes, the contribution of unstirred layers is minimized in the pressure relaxation mode: comparison with pressure clamp and high-pressure flowmeter. Plant Cell Environ. 30: 845-860.
Pubmed: Author and Title
Google Scholar: Author Only Title Only Author and Title

Lee J-Y, Wang X, Cui W, et al. A Plasmodesmata-Localized Protein Mediates Crosstalk between Cell-to-Cell Communication and Innate Immunity in Arabidopsis. The Plant Cell. 2011;23(9):3353-3373.
Pubmed: Author and Title
Google Scholar: Author Only Title Only Author and Title

Ma F, Peterson CA. 2001. Frequencies of plasmodesmata in Allium cepa L. roots: implications for solute transport pathways. J. Exp. Bot. 52: 1051-1061.
Pubmed: Author and Title
Google Scholar: Author Only Title Only Author and Title

Maule AJ. 2008. Plasmodesmata: structure, function and biogenesis. Curr. Opin. Plant Biol. 11(6): 680-686.
Pubmed: Author and Title
Google Scholar: Author Only Title Only Author and Title

Maurel C, Chrispeels MJ. 2001. Aquaporins. A molecular entry into plant water relations. Plant Physiol. 125(1): 135-138.
Pubmed: Author and Title
Google Scholar: Author Only Title Only Author and Title

McElrone AJ, Bichler J, Pockman WT, Addington RN, Linder CR, Jackson RB. 2007. Aquaporin-mediated changes in hydraulic conductivity of deep tree roots accessed via caves. Plant Cell Environ. 30(11): 1411-1421.
Pubmed: Author and Title
Google Scholar: Author Only Title Only Author and Title

Meunier F, Couvreur V, Draye X, Vanderborght J, Javaux M. 2017a. Towards quantitative root hydraulic phenotyping: novel mathematical functions to calculate plant-scale hydraulic parameters from root system functional and structural traits. J. of Mathematical Biol: 38 pp.
Pubmed: Author and Title
Google Scholar: Author Only Title Only Author and Title

Meunier F, Rothfuss Y, Bariac T, Biron P, Richard P, Durand J-L, Couvreur V, Vanderborght J, Javaux M. 2017b. Measuring and modeling hydraulic lift of Lolium multiflorum using stable water isotopes. Vadose Zone J.: 15 pp.
Pubmed: Author and Title
Google Scholar: Author Only Title Only Author and Title

Meunier F, Draye X, Vanderborght J, Javaux M, Couvreur V. 2017c. A hybrid analytical-numerical method for solving water flow equations in root hydraulic architectures. Appl. Math. Model. 52: 648-663.
Pubmed: Author and Title
Google Scholar: Author Only Title Only Author and Title

Parent B, Hachez C, Redondo E, Simonneau T, Chaumont F, Tardieu F. 2009. Drought and abscisic acid effects on aquaporin content translate into changes in hydraulic conductivity and leaf growth rate: A trans-scale approach. Plant Physiol. 149(4): 2000-2012.
Pubmed: Author and Title
Google Scholar: Author Only Title Only Author and Title

Pokhrel P, Gupta HV. 2010. On the use of spatial regularization strategies to improve calibration of distributed watershed models. Water Resour. Res. 46: 17 pp.
Pubmed: Author and Title
Google Scholar: Author Only Title Only Author and Title

Postma JA, Kuppe C, Owen MR, Mellor N, Griffiths M, Bennett MJ, Lynch JP, Watt M. 2017. OpenSimRoot: widening the scope and application of root architectural models. New Phytol. 215(3): 1274-1286.
Pubmed: Author and Title
Google Scholar: Author Only Title Only Author and Title

Pound MP, French AP, Wells DM, Bennett MJ, Pridmore TP. 2012. CellSeT: novel software to extract and analyze structured networks of plant cells from confocal images. The Plant Cell 24(4): 1353-1361.
Pubmed: Author and Title
Google Scholar: Author Only Title Only Author and Title

Pusch W, Woermann D. 1970. Study of the Interrelation Between Reflection Coefficient and Solute Rejection Efficiency Using a Strong Basic Anion Exchange Membrane. Ber. Bunsenges. phys. Chem., 74: 444-449
Pubmed: Author and Title
Google Scholar: Author Only Title Only Author and Title

Roberts AG, Oparka KJ. 2003. Plasmodesmata and the control of symplastic transport. Plant Cell Environ. 26(1): 103-124.
Pubmed: Author and Title
Google Scholar: Author Only Title Only Author and Title

Ross-Elliott TJ, Jensen KH, Haaning KS, Wager BM, Knoblauch J, Howell AH, Mullendore DL, Monteith AG, Paultre D, Yan D, Otero S, Bourdon M, Sager R, Lee J-Y, Helariutta Y, Knoblauch M, Oparka KJ. 2017. Phloem unloading in Arabidopsis roots is convective and regulated by the phloem-pole pericycle. eLife 6:e24125.
Pubmed: Author and Title
Google Scholar: Author Only Title Only Author and Title

Rygol J, Pritchard J, Zhu JJ, Tomos AD, Zimmermann U. 1993. Transpiration induces radial turgor pressure gradients in wheat and maize roots. Plant Physiol. 103: 493-500.
Pubmed: Author and Title
Google Scholar: Author Only Title Only Author and Title

Sanderson J. 1983. Water-uptake by different regions of the barley root. Pathways of radial flow in relation to development of the

endodermis. J. Exp. Bot. 34(140): 240-253.
Pubmed: Author and Title
Google Scholar: Author Only Title Only Author and Title

Schoppach R, Wauthelet D, Jeanguenin L, Sadok W. 2014. Conservative water use under high evaporative demand associated with smaller root metaxylem and limited trans-membrane water transport in wheat. Funct. Plant Bio. 41(3): 257-269.
Pubmed: Author and Title
Google Scholar: Author Only Title Only Author and Title

Schröder N, Lazarovitch N, Vanderborght J, Vereecken H, Javaux M. 2014. Linking transpiration reduction to rhizosphere salinity using a 3D coupled soil-plant model. Plant Soil 377(1-2): 277-293.
Pubmed: Author and Title
Google Scholar: Author Only Title Only Author and Title

Sevilem I, Miyashima S, Helariutta Y. 2013. Cell-to-cell communication via plasmodesmata in vascular plants. Cell Adhesion & Migration 7(1): 27-32.
Pubmed: Author and Title
Google Scholar: Author Only Title Only Author and Title

Sperry JS, Hacke UG, Oren R, Comstock JP. 2002. Water deficits and hydraulic limits to leaf water supply. Plant, Cell and Environment 25(2): 251-263.
Pubmed: Author and Title
Google Scholar: Author Only Title Only Author and Title

Steudle E, Boyer JS. 1985. Hydraulic resistance to radial water flow in growing hypocotyl of soybean measured by a new pressure-perfusion technique. Planta 164(2): 189-200.
Pubmed: Author and Title
Google Scholar: Author Only Title Only Author and Title

Steudle E, Frensch J. 1989. Osmotic responses of maize roots. Planta 177(3): 281-295.
Pubmed: Author and Title
Google Scholar: Author Only Title Only Author and Title

Steudle E, Jeschke WD. 1983. Water transport in barley roots : Measurements of root pressure and hydraulic conductivity of roots in parallel with turgor and hydraulic conductivity of root cells. Planta 158: 237-248.
Pubmed: Author and Title
Google Scholar: Author Only Title Only Author and Title

Steudle E, Oren R, Schulze ED. 1987. Water transport in maize roots - Measurement of hydraulic conductivity, solute permeability, and of reflection coefficients of excised roots using the root pressure probe. Plant Physiol. 84(4): 1220-1232.
Pubmed: Author and Title
Google Scholar: Author Only Title Only Author and Title

Steudle E, Peterson CA. 1998. How does water get through roots? J. Exp. Bot. 49(322): 775-788.
Pubmed: Author and Title
Google Scholar: Author Only Title Only Author and Title

Terry BR, Robards AW. 1987. Hydrodynamic radius alone govems the mobility of molecules through plasmodesmata. Planta 171: 145-157.
Pubmed: Author and Title
Google Scholar: Author Only Title Only Author and Title

Tornroth-Horsefield S, Wang Y, Hedfalk K, Johanson U, Karlsson M, Tajkhorshid E, Neutze R, Kjellbom P. 2006. Structural mechanism of plant aquaporin gating. Nature 439(7077): 688-694.

Tournaire-Roux C, Sutka M, Javot H, Gout E, Gerbeau P, Luu DT, Bligny R, Maurel C. 2003. Cytosolic pH regulates root water transport during anoxic stress through gating of aquaporins. Nature 425(6956): 393-397.

Tyree MT. 1968. Determination of transport constants of isolated Nitella cell walls. Canad. J. Bot. 46: 317-327.
Pubmed: Author and Title
Google Scholar: Author Only Title Only Author and Title

Varney GT, Canny MJ. 1993. Rates of water-uptake into the mature root-system of maize plants. New Phytol. 123(4): 775-786.
Pubmed: Author and Title
Google Scholar: Author Only Title Only Author and Title

Von Wangenheim D, Goh T, Dietrich D, Bennett MJ. 2017. Plant biology: building barriers... in Roots. Current Biology 27(5): R172-R174.
Pubmed: Author and Title
Google Scholar: Author Only Title Only Author and Title

Warmbrodt RD. 1985. Studies on the root of Zea mays L.-structure of the adventitious roots with respect to phloem unloading. Bot. Gaz. 146(2): 169-180.
Pubmed: Author and Title
Google Scholar: Author Only Title Only Author and Title

Ye Q, Steudle E. 2006. Oxidative gating of water channels (aquaporins) in corn roots. Plant Cell Environ. 29(4): 459-470.
Pubmed: Author and Title
Google Scholar: Author Only Title Only Author and Title

Zarebanadkouki M, Kroener E, Kaestner A, Carminati A. 2014. Visualization of root water uptake: Quantification of deuterated water transport in roots using neutron radiography and numerical modeling. Plant Physiol.
Pubmed: Author and Title
Google Scholar: Author Only Title Only Author and Title

Zarebanadkouki M, Meunier F, Couvreur V, Cesar J, Javaux M, Carminati A. 2016. Estimation of the hydraulic conductivities of lupine roots by inverse modelling of high-resolution measurements of root water uptake. Ann. Bot.
Pubmed: Author and Title
Google Scholar: Author Only Title Only Author and Title

Zhu GL, Steudle E. 1991. Water transport across maize roots: simultaneous measurement of flows at the cell and root level by double pressure probe technique. Plant Physiol. 95(1): 305-315.
Pubmed: Author and Title
Google Scholar: Author Only Title Only Author and Title

Zimmermann HM, Hartmann K, Schreiber L, Steudle E. 2000. Chemical composition of apoplastic transport barriers in relation to radial hydraulic conductivity of corn roots (Zea mays L.). Planta 210: 302-311.
Pubmed: Author and Title
Google Scholar: Author Only Title Only Author and Title

Zwieniecki MA, Thompson MV, Holbrook MN. 2002. Understanding the hydraulics of porous pipes: Tradeoffs between water uptake and root length utilization. J. Plant Growth Regul. 21: 315-323.
Pubmed: Author and Title
Google Scholar: Author Only Title Only Author and Title